Fluid Phase Equilibria 457 (2018) 18–37

Contents lists available at ScienceDirect

Fluid Phase Equilibria

journal homepage: www.elsevier.com/locate/fluid

Computation and analysis of surfaces and lines of three-phase equilibrium in ternary systems: Application illustrated for a $CO_2(1)+H_2O(2)+2\text{-propanol}(3)$-like system

Gerardo O. Pisoni [a, b], Martín Cismondi [a], Marcelo S. Zabaloy [b, *]

[a] Facultad de Ciencias Exactas, Físicas y Naturales, Universidad Nacional de Córdoba (UNC), Instituto de Investigación en Ingeniería de Procesos y Química Aplicada (IPQA), CONICET, Av. Vélez Sarsfield 299, X5000JJC Córdoba. Argentina
[b] Departamento de Ingeniería Química, Universidad Nacional del Sur (UNS), Planta Piloto de Ing. Química (PLAPIQUI), CONICET, CC 717, 8000 Bahía Blanca, Argentina

ARTICLE INFO

Article history:
Received 24 May 2017
Received in revised form
11 October 2017
Accepted 16 October 2017
Available online 17 October 2017

Keywords:
Ternary phase equilibrium
Three-phase lines
Three-phase surfaces
Equation of state
Calculation algorithms
High pressure

ABSTRACT

In this work the rich phenomenology of the ternary three-phase equilibrium is studied for a $CO_2(1)+H_2O(2)+2\text{-propanol}(3)$-like system which presents a highly complex behavior. This is done through computations carried out over wide ranges of conditions using a model of the equation of state type. The developed computation and analysis strategies are applicable to any ternary system as described by any equation of state model, chosen for representing real systems having a high degree of complexity in their phase behavior. A systematic identification of phase equilibrium objects (or points) from which ternary three-phase lines (T-3PLs) originate is performed. Such points are used to start the computation of a variety of T-3PLs. Several computed T-3PLs are used to visualize a number of ternary three-phase surfaces (T-3PSs). Besides, the boundaries of the T-3PSs are established. A strategy to start the calculation of a T-3PL is proposed for each type of originating point. In addition, with the aim of avoiding convergence problems, a numerical continuation method is used to calculate complete T-3PLs. The visualization of 3D projections of T-3PSs in the temperature-pressure-fugacity space is proposed. This way of looking at the T-3PSs is of much help in the understanding on how they behave and interrelate. The results suggest, among other interesting conclusions, the possibility of continuous transitions from T-3PSs of a given type to T-3PSs of a different type.

1. Introduction

A type of fluid phase equilibrium of special interest is the three-phase equilibrium (3PE) (see, e.g., refs [1] and [2]). The accurate reproduction of experimental 3PE is a stringent test for thermodynamic models for multicomponent mixtures, mainly if the multicomponent system considered is highly non-ideal. If this test is passed by a given model, for the case of ternary systems, then, the user should be more confident about its performance for multicomponent systems. The calculation of the ternary 3PE (T-3PE) is also a stringent test for computation algorithms. This is because the behavior of continuous sets of three-phase equilibria may be of considerable complexity. Reliable algorithms are also needed in the process of fitting the model interaction parameters.

A ternary system can exhibit a wide variety of three-phase equilibria. Different 3PE points may belong to the same ternary three-phase surface (T-3PS) or to different T-3PSs. In turn, the topology of a T-3PS could be complex and difficult to interpret. In particular, to be aware of the variety of equilibrium phenomena of potential occurrence, when a continuous set of ternary three-phase equilibria comes to an end, is crucial to interpret properly T-3PE experimental results obtained in the laboratory, and even to study failures of computation algorithms.

Important fluid phase equilibrium diagrams are those that are made of univariant equilibrium lines and invariant equilibrium points. We name such diagrams phase equilibrium “characteristic maps”, more specifically, “Binary characteristic map” (B-CM) and “ternary characteristic map” (T-CM), for binary and ternary systems, respectively. A point of a univariant equilibrium line becomes defined when a single degree of freedom is specified. This means

* Corresponding author.
E-mail address: mzabaloy@plapiqui.edu.ar (M.S. Zabaloy).

https://doi.org/10.1016/j.fluid.2017.10.011
0378-3812/

that it is 'necessary' to specify the value of a variable of the system to establish the equilibrium. Actually, and more generally, specifying a relationship between a sub-set of the variables of the system is also a way of spending the single degree of freedom available. On the other hand, an invariant equilibrium point is a point with zero degrees of freedom.

Scott and van Konynenburg [3] described a variety of B-CMs, and proposed a classification for their behavior. This classification is based on the observation, in the pressure-temperature plane, of the topology of computed univariant equilibrium lines. Such lines were calculated in Ref. [3] using the van der Waals equation of state (EoS). Cismondi and Michelsen [4] proposed a methodology for the calculation of B-CMs as those shown in Ref. [3].

The equilibrium behavior of the binary system is defined over the entire ranges of temperature, pressure and composition once all the parameters values of the EoS are set. The univariant lines that compose the B-CM are binary three-phase lines (B-3PLs), binary critical lines (B-CLs) and binary azeotropic lines; while the invariant points involved are binary critical end points (B-CEPs) and binary azeotropic end points. Tables 1 and 2 provide, respectively, the meaning of the acronyms used in this work, and the description of the physical situation for a variety of phase equilibrium objects. Not all binary behaviors have three-phase equilibrium. In addition, the (univariant) vapour-liquid equilibrium lines of the pure compounds and their respective (invariant) critical points are included in the B-CM.

When going from binary to ternary systems, a ternary fluid phase equilibrium characteristic map arises (T-CM), and the behavior of the 3PE becomes considerably more complex. Clearly, the binary 3PE has a single degree of freedom which implies that a continuous set of binary 3PE points is a line (or hyper-line). In contrast, the 3PE in a ternary system has two degrees of freedom. This implies that an unrestricted continuous set of ternary 3PE points is a surface (or hyper-surface) and not a line, as it is in binary systems. Consequently, the ternary 3PE is not a thermodynamic object that contributes to the ternary characteristic map (T-CM).

Table 1
Acronyms used in this work and in Ref. [10–12].

Acronym	Meaning	# of phases	# of crit. phases
P-VPL	Pure (compound) vapour-pressure line	2	
B-3PP	Binary three-phase point	3	
B-3PL	Binary three-phase line (locus of B-3PPs)	3	
T-3PP	Ternary three-phase point	3	
T-3PL	Ternary three-phase line (locus of T-3PPs)	3	
T-3PS	Ternary three-phase surface	3	
T-4PP	Ternary four-phase point	4	
T-4PL	Ternary four-phase line (locus of T-4PPs)	4	
P-CP	Pure critical point	1	1
B-CP	Binary-critical point	1	1
B-CL	Binary-critical line (locus of B-CPs)	1	1
B-CEP	Binary-critical end point	2	1
T-CEP	Ternary-critical end point	2	1
T-CEL	Ternary-critical end line (locus of T-CEPs)	2	1
T-CEP-4PL	Ternary-critical end point of a four phase line	3	1
T-TCP	Ternary-tricritical point (this is a synonym of T-TCEP)	1	
T-TCEP	Ternary-tricritical end point (this is a synonym of T-TCP)	1	
T-CM	Ternary characteristic map (characteristic map of the fluid phase behavior of a ternary system)		
B-CM	Binary characteristic map (characteristic map of the fluid phase behavior of a binary system)		
NCM	Numerical Continuation Method		
3PE	Three-phase equilibrium	3	
T-3PE	Ternary Three-Phase Equilibrium	3	

Table 2
Thermodynamic objects present in a ternary characteristic map (T-CM).

	Type of thermodynamic object	No. of components	Phase condition
Univariant lines	Pure vapour pressure line (P-VPL)	1	L + V
	Binary three-phase line (B-3PL)	2	L + L + V
	Binary critical line (B-CL)	2	Critical phase (L1 = L2 or L = V)
	Binary Azeotropic Line	2	L + V (phases with same composition)
	Ternary critical end Line (T-CEL)	3	Critical phase + non-critical phase ((L1 = L2)+V or L1+(L2 = V))
	Ternary four phase Line (T-4PL)	3	L + L + L + V
	Ternary Azeotropic Line	3	L + V (phases with same composition)
Invariant Points	Pure Critical Point (P-CP)	1	Critical phase (L = V)
	Binary Critical End Point (B-CEP)	2	Critical phase + non critical phase ((L1 = L2)+V or L1+(L2 = V))
	Binary Azeotropic end Point	2	Two phases with same composition may become critical (L = V), or can be infinitely diluted in a component, or may become unstable by the appearance of a third phase at equilibrium with the azeotropic phases (L + L + V) [13]
	Ternary Critical End Point of a Four Phase Line (T-CEP-4PL)	3	A T-CEP-4PL is an endpoint of a T-4PL, where two of the four phases become critical. (e.g., L1+L2+(L3 = V), or, e.g., L1+(L2 = L3)+V, etc.)
	Ternary Tricritical Point (T-TCP) or Ternary Tricritical End Point (T-TCEP)	3	In a T-TCP three non-critical phases at equilibrium become critical simultaneously. (L1 = L2 = V)
	Ternary Azetropic end Point (T-AEP)	3	Not considered in this work.

L = Liquid; V=Vapour.

However, the thermodynamic objects which are the boundaries of a ternary three-phase surface (T-3PS) are ternary univariant lines which do contribute to the T-CM.

A variety of works that study the ternary three-phase equilibrium (T-3PE) phenomenon can be found in the bibliography.

Di Andreth et al. [5] analyze the T-3PE in a pressure range at constant temperature (333 K) for the *CO_2+H_2O+2-propanol* fluid system (Figs. 5 and 6 in Ref. [5]). The authors show the *"molar volume versus pressure"* projection of the 333 K T-3PE isotherm (L1 + L2 + G, Fig. 7 in Ref. [5]). Such diagram is one of the possible 3D projections of the 333 K T-3PE line (T-3PL) (or hyper-line). It can be seen in Fig. 7 of ref. [5] that the molar volumes of the liquid phases L1 and L2 are identical at a given pressure (lowest T-3PE pressure), i.e., two of the three phases at equilibrium (the two liquid phases) become critical ((L1 = L2) + G) when moving along the T-3PL from higher to lower pressures. This behavior also occurs to the phases L2 and G, but at the highest T-3PE pressure, which results in a second situation where a critical phase is at equilibrium with a noncritical phase (L1 + (L2 = G)). Both physical situations set the termination of the T-3PL. Thus, they are identified as "terminal points" or "endpoints" ((L1 = L2) + G and L1 + (L2 = G)) of the T-3PL. More specifically, these points are named ternary critical endpoints (T-CEPs, see Tables 1 and 2). In Ref. [5], the authors do not analyze the evolution with temperature of T-3PLs and T-CEPs.

Gregorowicz et al. [6] reported, for the system ethylene + propane + n-eicosane, several experimental T-CEPs, which were shown in the pressure-temperature plane (Fig. 5 in Ref. [6]). Such T-CEPs describe a couple of special equilibrium lines which are boundaries of the T-3PS. Such lines are named 'ternary critical end lines' (T-CELs, see Tables 1 and 2). However, in general terms, the T-

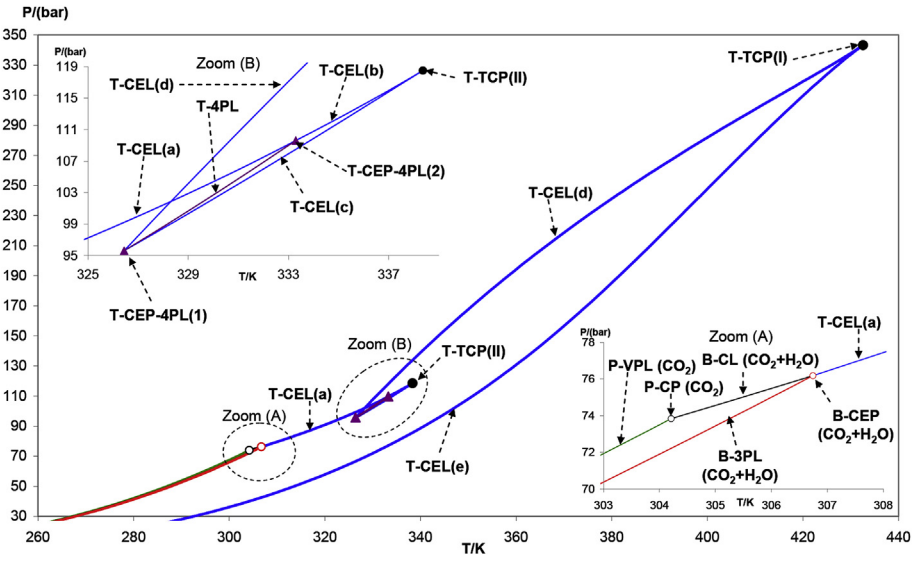

Fig. 1. Part of the ternary fluid phase equilibrium characteristic map (T-CM) calculated for the *CO_2(1)+H_2O(2)+2-propanol(3)*[A] system using SRK-EOS with parameters from Tables 3 and 4. Labels: P-VPL: Pure (compound) vapour-pressure line. P-CP: Pure critical point. B-3PL: Binary three-phase line. B-CL: Binary-critical line. B-CEP: Binary-critical end point. T-CEL: Ternary-critical end line. T-CEP-4PL: Ternary-critical end point of a four phase line. T-TCP: Ternary-tricritical point. T-4PL: Ternary four-phase line. Phase condition associated to labels: Table 2. Important: See note in Table 4.

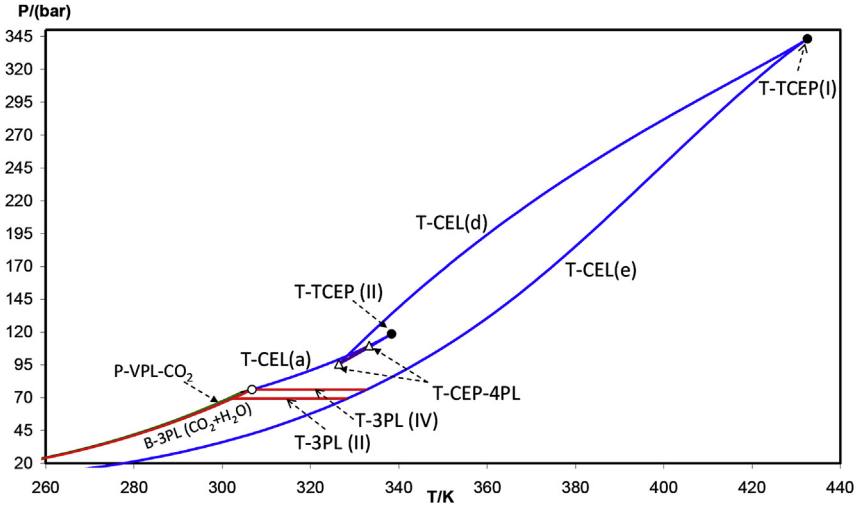

Fig. 2. Pressure-Temperature projection of the T-CM computed for system *CO_2(1)+H_2O(2)+2-propanol(3)*[A], with indication of location and extent of the isobaric T-3PLs: T-3PL(II) and T-3PL(IV). Model: SRK-EoS (see Table 4). Empty circle: B-CEP. Labels: P-VPL: Pure (compound) vapour-pressure line. B-3PL: Binary three-phase line. B-CEP: Binary-critical end point. T-CEL: Ternary-critical end line. T-3PL: Ternary three-phase line. T-CEP-4PL: Ternary-critical end point of a four phase line. T-TCEP: Ternary-tricritical end point. T-CM: ternary fluid phase equilibrium characteristic map. Phase condition associated to labels: Table 2. Important: See note in Table 4.

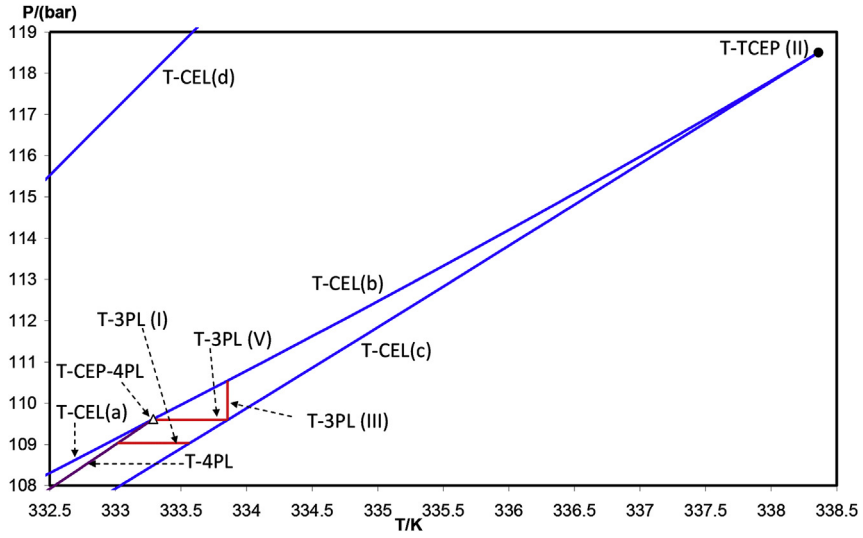

Fig. 3. Zoom of Fig. 2, with indication of location and extent of the isobaric T-3PLs: T-3PL(I) and T-3PL(V), and of the isothermal T-3PL(III). System: *CO_2(1)+H_2O(2)+2-propanol(3)* [A]. Labels: T-CEL: Ternary-critical end line. T-3PL: Ternary three-phase line. T-CEP-4PL: Ternary-critical end point of a four phase line. T-TCEP: Ternary-tricritical end point. T-4PL: Ternary four-phase line. Phase condition associated to labels: Table 2. Important: See note in Table 4.

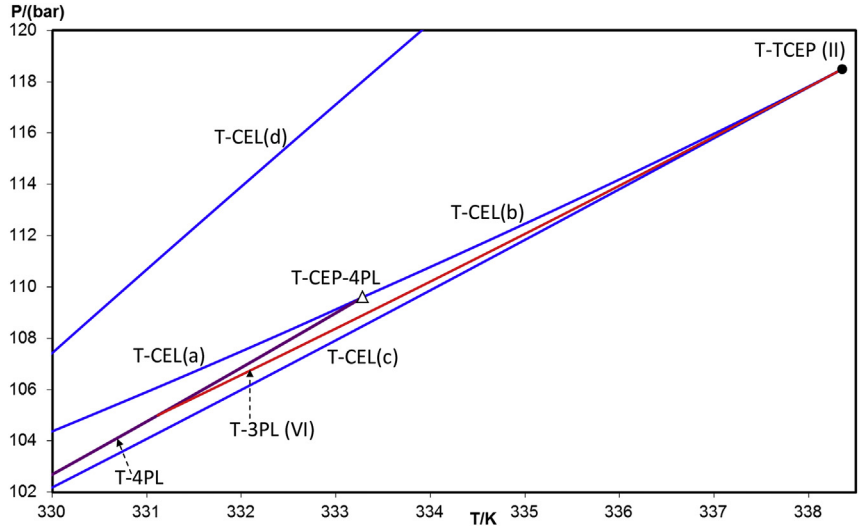

Fig. 4. Zoom of Fig. 1, with indication of location and extent of the T-3PL(VI). System: *CO_2(1)+H_2O(2)+2-propanol(3)* [A]. Labels: T-CEL: Ternary-critical end line. T-3PL: Ternary three-phase line. T-CEP-4PL: Ternary-critical end point of a four phase line. T-TCEP: Ternary-tricritical end point. T-4PL: Ternary four-phase line. Phase condition associated to labels: Table 2. Important: See note in Table 4.

CELs are not the only type, of possible boundaries involving only fluid phases, of a T-3PS. This was not discussed by Gregorowicz et al. [6].

Winkler and Stephan [7] reported, for the *CO_2+H_2O+1-butanol* system, experimental information on three- and four-phase equilibria and on critical lines and critical endpoints. They also used an equation of state (EoS) to complete the description of the phase behavior in regions experimentally not accessible. In Fig. 9 of ref [7] it can be seen that, in addition to the T-CELs, a ternary four phase equilibrium line (T-4PL) is also a possible boundary of a T-3PS. The work of ref [7] covers limited ranges of temperature and pressure, i.e., from 296 to 315 K and from 5.8 to 11 MPa. Therefore, boundaries of T-3PSs of types different from T-CELs or T-4PLs were not considered in Ref. [7]. On the other hand, the relationship between a T-4PL and the four T-3PSs stemming from it is not discussed by the authors in such terms.

Adrian et al. [8] studied the phase equilibrium behavior of the *CO_2+H_2O + Propionic Acid* and *CO_2+H_2O+2-propanol* systems. The authors experimentally found the ranges of existence of the T-3PE. Qualitative prism diagrams were used to explain the evolution with pressure of the T-3PE at constant temperature (e.g., Fig. 1 in Ref. [8]). In addition, T-CEPs, tricritical points (T-TCPs, Table 1), and special four-phase points were established as points of the T-3PS boundaries (Figs. 3 and 4 in Ref. [8]). However, the study was done in a relatively narrow range of pressure (5–11 MPa) and only for three different temperatures (298 K, 313 K and 333 K) [8]. Later, in a related work, Adrian et al. [9] found the regions where the T-3PE exists for the *CO_2+H_2O+1-propanol* system. They detected different T-3PSs, which however develop (again) in narrow ranges of pressure and temperature. The authors [9] did not analyze in a comprehensive way the topology of each T-3PS. They did not discuss either, in the way we do in this work, how the four-phase

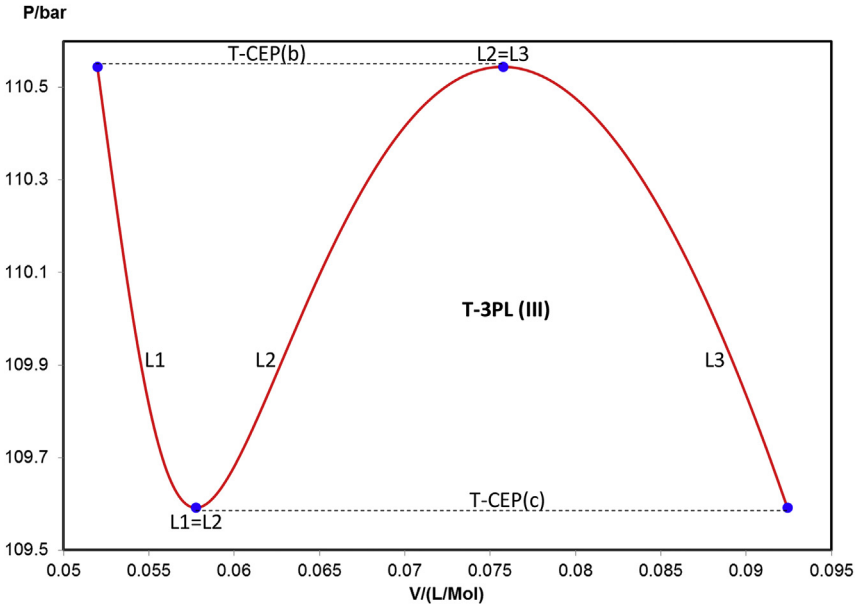

Fig. 5. Pressure-Molar Volume projection of the calculated isothermal T-3PL(III) (T = 333.85 K, see Fig. 3). System: *CO_2(1)+H_2O(2)+2-propanol(3)* [A]. Model: SRK-EoS (see Table 4). Labels: T-3PL: Ternary three-phase line. T-CEP: Ternary-critical end point. Phase condition associated to labels: Table 2. Important: See note in Table 4.

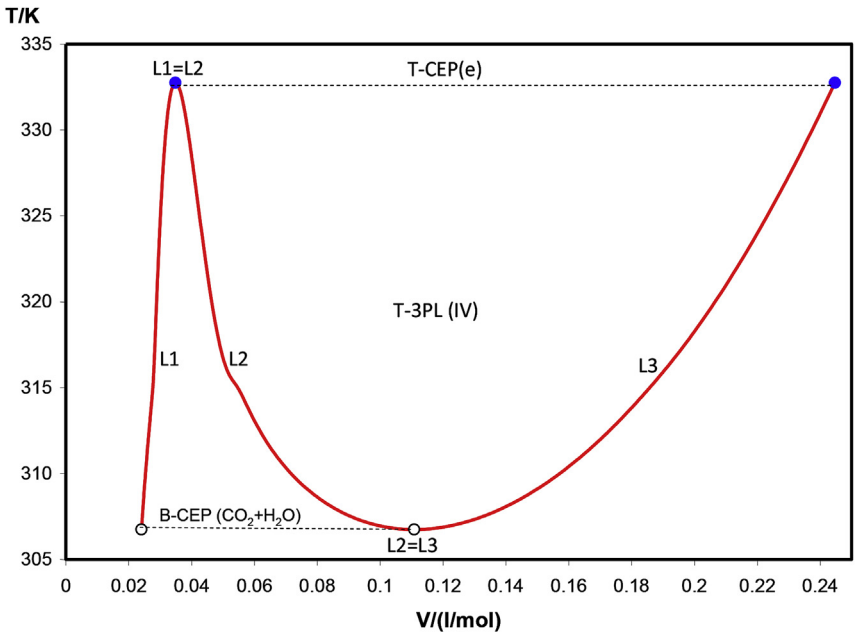

Fig. 6. Temperature-Molar Volume projection of the calculated isobaric T-3PL(IV) (P = 76.17 bar). See Fig. 2. System: *CO_2(1)+H_2O(2)+2-propanol(3)* [A]. Model: SRK-EoS (see Table 4). Labels: T-3PL: Ternary three-phase line. T-CEP: Ternary-critical end point. B-CEP: Binary-critical end point. Phase condition associated to labels: Table 2. Important: See note in Table 4.

equilibrium relates to the T-3PSs.

Details on phase equilibrium calculation procedures are scarce in the works quoted above.

To better understand the behavior of the ternary three-phase equilibrium, it is convenient to know the complete fluid phase equilibrium "ternary characteristic map" (T-CM). For ternary systems, Pisoni et al. [10] carried out a study analogous in many ways to that of Scott and van Konynenburg [3] for binaries. In such work [10], the thermodynamic objects that compose the T-CM are established and properly named (such objects are univariant lines and invariant points for ternary systems). In addition, the authors defined and implemented [10] algorithms to compute complete T-CMs. From the computed T-CMs in Ref. [10] (Figs. 2–14 in Ref. [10]), it can be deduced that the ternary three-phase behavior is considerably more complex than the binary three-phase behavior. This is related to the previously mentioned fact that the T-3PE is described by hyper-surfaces and not by hyper-lines as it is the case for the binary three-phase equilibrium. In the context of phase equilibria computations, once the T-CM has been generated, the thermodynamic objects defining the boundaries of the T-3PSs become available. The information that this boundaries provide is very useful for calculating sets of ternary three-phase equilibrium

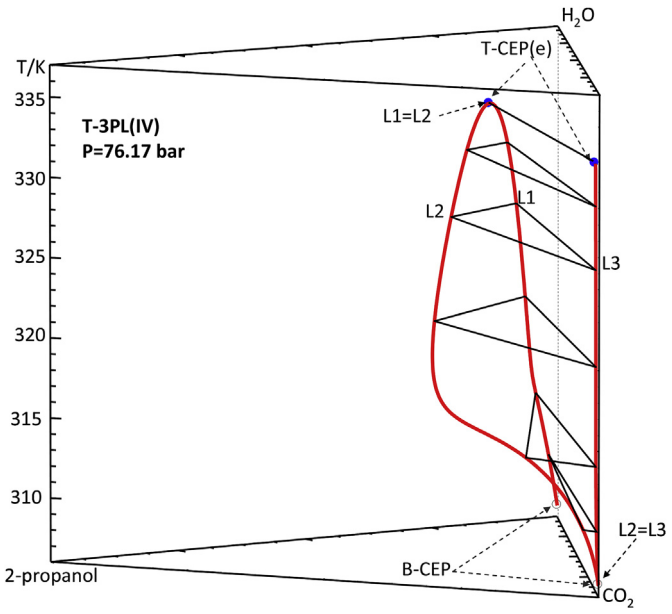

Fig. 7. Temperature-Mole Fraction projection of the calculated isobaric T-3PL(IV) presented in a ternary Gibbs prism. System: *CO_2(1)+H_2O(2)+2-propanol(3)* [A]. Model: SRK-EoS (see Table 4). Concentration scale: mole fraction. Five three-phase equilibrium points are indicated as horizontal triangles of variable area, whose sides are the equilibrium tie-lines. Labels: T-3PL: Ternary three-phase line. T-CEP: Ternary-critical end point. B-CEP: Binary-critical end point. Phase condition associated to labels: Table 2. Important: See note in Table 4.

lines (T-3PLs) which describe the topology of the system's T-3PSs.

A given T-3PE thermodynamic object, such as ternary three-phase equilibrium points (T-3PPs), T-3PLs and T-3PSs, is described by a number of variables (pressure, temperature, component mole fractions, etc.). For this reason, occasionally the terms "hyper-point" or "hyper-line" or "hyper-surface" are used. The multidimensional nature of T-3PLs and T-3PSs imply the existence of several projections for these thermodynamic objects, e.g., pressure vs. mole fraction, temperature vs. density, etc.

The goals of the present work are the following: [a] to propose and test robust calculation methodologies to compute ternary three-phase equilibrium lines (T-3PLs), to be used for building T-3PSs, and, [b] to show how the study of the topology and behavior of computed T-3PSs can be conducted in a quite comprehensive way, for highly non-ideal systems. Of particular interest in this study is to understand how the ternary four-phase equilibria and the T-3PSs interrelate. This is done with the help of a thermodynamic model used to describe a couple of model systems. The use of model systems makes possible to study the ternary phase equilibrium with no limitations in the ranges of conditions (as those associated to experimental equipment), a no interference of solids (which limits the range of existence of fluid phase equilibria in experimental studies). The scientific community has a long tradition in using model systems to improve the understanding of phase equilibria (e.g., ref [3]).

We anticipate now that to compute a ternary three-phase point (T-3PP), the corresponding equilibrium conditions are solved using the Newton-Raphson method; and that to compute a complete T-3PL, a numerical continuation method (NCM) is used. The NCM uses crucial information on a previous, already converged, T-3PP (of the T-3PL being built) to generate excellent initial estimates for the system variables of the next T-3PP to be computed, and to identify the optimum variable to be specified for calculating such next T-3PP.

2. Ternary characteristic map (T-CM)

The fluid phase equilibrium T-CM is constituted exclusively by "univariant equilibrium lines" and "invariant points". These lines and points are those found in the three related B-CMs, plus those for which the three components are present. The T-CM provides the boundaries of the system's T-3PSs.

The terminology for the thermodynamic objects present in T-CMs is defined in Table 2 (also see Table 1) which, among other pieces of information, reports the number of components and features of coexisting phases, for every listed thermodynamic object.

To illustrate how a T-CM may look like, Fig. 1 shows a part of a T-CM for the *CO_2+H_2O+2-propanol*[A] system, computed using the SRK-EOS [14] with parameters from Tables 3 and 4. In this figure, the pure vapour pressure line (P-VPL) of *CO_2* is shown to extend up to the pure critical point (P-CP) for this compound (see the Zoom

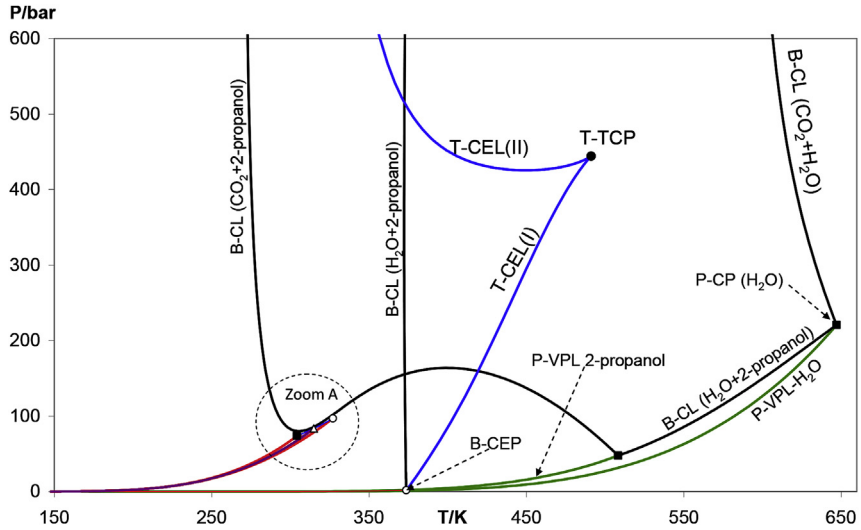

Fig. 8. Pressure-Temperature projection of the T-CM computed for system *CO_2(1)+H_2O(2)+2-propanol(3)* [B]. Model: SRK-EoS (see Table 4). Labels: T-CM: ternary fluid phase equilibrium characteristic map. P-VPL: Pure (compound) vapour-pressure line. P-CP: Pure critical point. B-CL: Binary-critical line. B-CEP: Binary-critical end point. T-CEL: Ternary-critical end line. T-TCP: Ternary-tricritical point. Phase condition associated to labels: Table 2. Important: See note in Table 4.

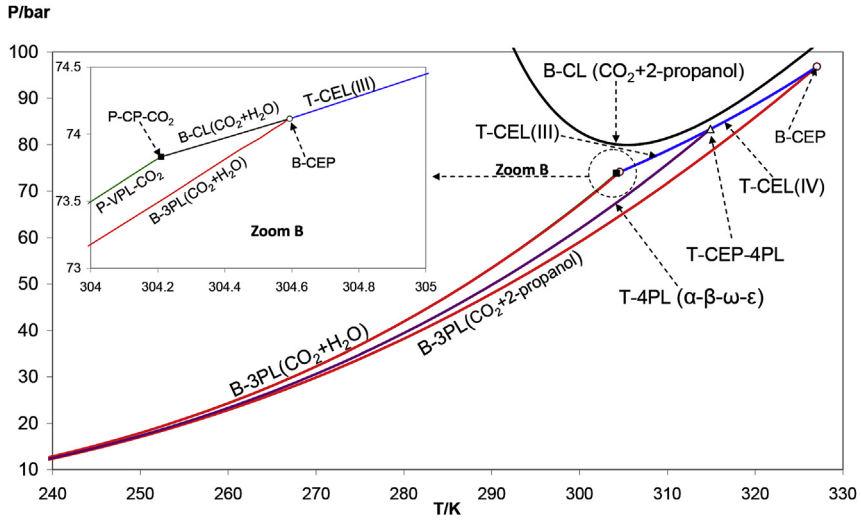

Fig. 9. Zoom of Fig. 8. Labels: P-VPL: Pure (compound) vapour-pressure line. P-CP: Pure critical point. B-3PL: Binary three-phase line. B-CL: Binary-critical line. B-CEP: Binary-critical end point. T-CEL: Ternary-critical end line. T-CEP-4PL: Ternary-critical end point of a four phase line. T-4PL: Ternary four-phase line. Phase condition associated to labels: Table 2. Important: See note in Table 4.

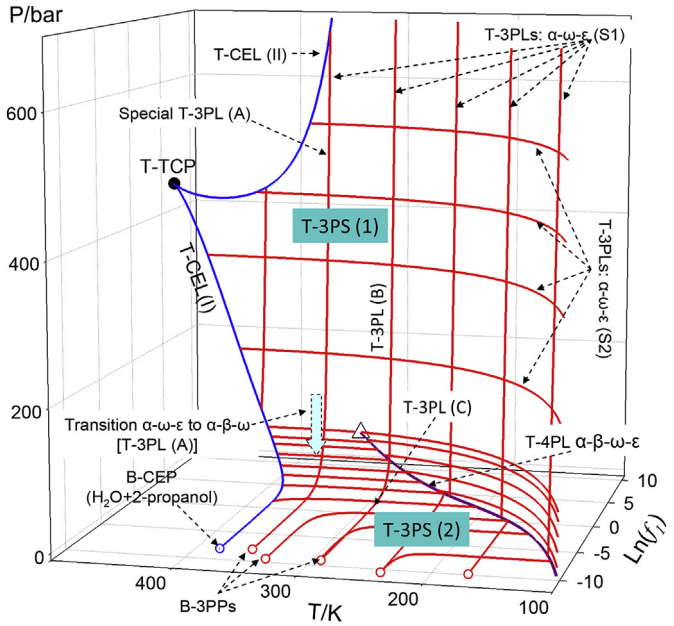

Fig. 10. Pressure-Temperature-ln($\hat{f}_1$) projection of several T-3PLs computed for the $CO_2(1)$+$H_2O(2)$+2-propanol(3) [B] system. These T-3PLs (together with the T-4PL and other boundaries) outline the T-3PSs (1) and (2). Model: SRK-EoS (see Table 4). Fugacity units: bar. The "B-3PPs" correspond to system H_2O+2-propanol. The phase combination for the T-3PS (2) is α−β−ω. Triangle: T-CEP-4PL. Labels: B-CEP: Binary-critical end point. B-3PP: Binary three-phase point. T-3PL: Ternary three-phase line. T-CEL: Ternary-critical end line. T-CEP-4PL: Ternary-critical end point of a four phase line. T-TCP: Ternary-tricritical point. T-4PL: Ternary four-phase line. T-3PS: Ternary three-phase surface. Phase condition associated to labels: Table 2. Important: See note in Table 4.

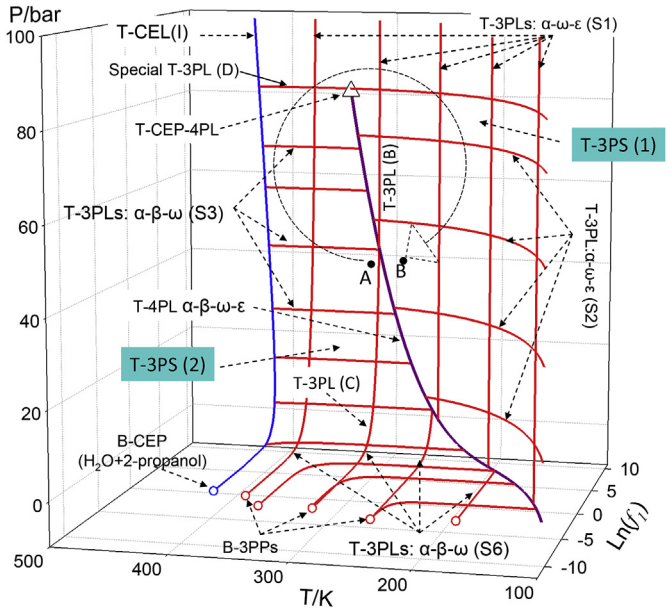

Fig. 11. Zoom of Fig. 10. System: $CO_2(1)$+$H_2O(2)$+2-propanol(3) [B]. The "B-3PPs" correspond to system H_2O+2-propanol. Labels: B-CEP: Binary-critical end point. B-3PP: Binary three-phase point. T-3PL: Ternary three-phase line. T-CEL: Ternary-critical end line. T-CEP-4PL: Ternary-critical end point of a four phase line. T-4PL: Ternary four-phase line. T-3PS: Ternary three-phase surface. Phase condition associated to labels: Table 2. Important: See note in Table 4.

(A) insert in the lower right corner of Fig. 1). From the P-CP, a binary critical line (B-CL) of the CO_2+H_2O system begins [Zoom (A)], and then ends at a binary critical end point (B-CEP) for this system [Zoom (A)]. From the B-CEP, two equilibrium lines begin, i.e., the binary three-phase line (B-3PL) of the CO_2+H_2O system [Zoom (A)] and a first ternary critical end line, i.e., T-CEL(a). See Zoom (A) and Zoom(B). Zoom(B) is the insert in the top left corner of Fig. 1, which corresponds to higher temperatures than Zoom(A). The T-CEL(a) extends up to the ternary critical end point of a four phase line T-CEP-4PL(2) [Zoom (B), see Tables 1 and 2]. From this last point, a second T-CEL(b) [Zoom (B)] begins, and then ends at the ternary tricritical point T-TCP(II) [in Zoom (B), see Tables 1 and 2]. The third T-CEL(c) extends between the T-TCP(II) and the T-CEP-4PL(1) [in Zoom (B)]. Between the two T-CEPs-4PL a T-4PL develops [in Zoom (B), see Tables 1 and 2]. From the T-CEP-4PL(1) the T-CEL(d) begins, and ends at an another ternary tricritical point, i.e., T-TCP(I) (see main Fig. 1). Finally, from the T-TCP(I) the T-CEL(e) begins, which extends towards low pressures and temperatures.

Fig. 1 presents only a part of the complete T-CM (such complete T-CM for this system is shown in Fig. 12 of reference [10]). The level

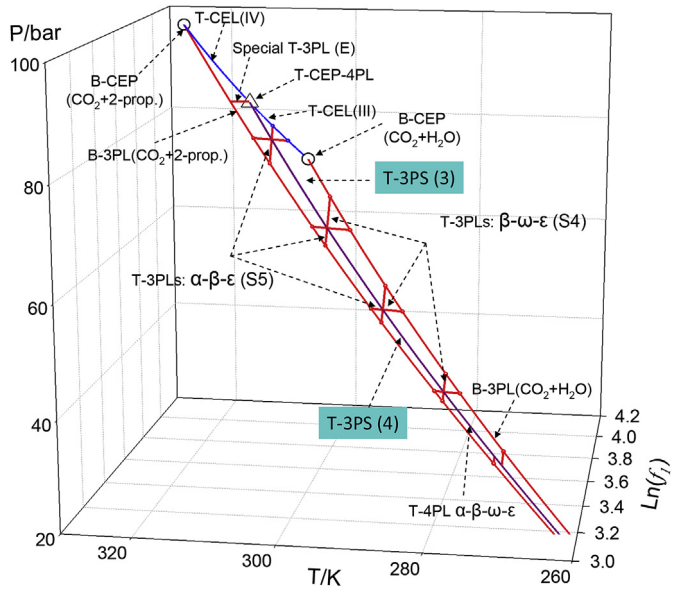

Fig. 12. Pressure-Temperature-ln($\hat{f}_1$) projection of several T-3PLs computed for the *CO_2(1)+H_2O(2)+2-propanol(3)* [B] system. These T-3PLs (together with the T-4PL and other boundaries) outline the T-3PSs (3) and (4). Model: SRK-EoS (see Table 4). Fugacity units: bar. Labels: B-CEP: Binary-critical end point. B-3PL: Binary three-phase line. T-3PL: Ternary three-phase line. T-CEL: Ternary-critical end line. T-CEP-4PL: Ternary-critical end point of a four phase line. T-4PL: Ternary four-phase line. T-3PS: Ternary three-phase surface. Phase condition associated to labels: Table 2. Important: See note in Table 4.

of complexity of a computed T-CM depends on the chosen thermodynamic model, and on the pure compound and interaction parameters values. In Ref. [10] a variety of T-CMs were computed, which presented from simple to very complex topologies. Ref. [10] provides a flowchart for the T-CM calculation algorithm.

3. Boundaries of a T-3PS

From section 1, the possible types of boundary lines of a T-3PS are: T-CELs, T-4PLs and B-3PLs (Fig. 1). Besides, the following types of invariant points may be located on the boundaries of a T-3PS: T-CEPs-4PL, T-TCPs and the B-CEPs (Fig. 1).

At a T-CEP-4PL, a T-4PL and a couple of T-CELs meet (Fig. 1), bounding, each T-CEL, a different T-3PS. At a T-TCP, two T-CELs of the same T-3PS meet (Fig. 1). At a B-CEP, a B-3PL and a T-CEL meet (Fig. 1), being both lines boundaries of the same T-3PS. In conclusion, an invariant point belonging to a T-3PS is in all cases a point where two boundary lines of such T-3PS meet.

The lines T-CEL, T-4PL and B-3PL, and the points T-CEP-4PL, T-TCP and B-CEP, have all a phase condition related to that of the ternary three-phase equilibrium. Thus, it is possible to start off the calculation of a T-3PL using information from these lines and points. In other words, the knowledge of computed boundaries of a T-3PS makes possible to calculate a set of T-3PLs, which define (or outline) the topology of such T-3PS.

Section 5 describes a strategy to start the calculation of a T-3PL from information taken from an already converged T-4PP (this is a point of a T-4PL, which is a boundary of a T-3PS). Appendix A does the same for the other thermodynamic objects considered above (e.g., B-CEP).

The next section describes the thermodynamic conditions that must be satisfied to compute a T-3PP. It also describes, briefly, the coupled numerical continuation method used to compute a complete T-3PL.

4. Ternary three-phase equilibrium: T-3PPs, T-3PLs and T-3PSs

A T-3PS can be basically described by an appropriate set of a large enough number of T-3PLs. In turn, a T-3PL is a continuous set of T-3PPs (a T-3PP has two degrees of freedom). It is convenient to have available a methodology that makes possible to compute a complete T-3PL in a single run.

To compute a T-3PP, the iso-fugacity condition for each component in the three phases at equilibrium must be satisfied. Also, the pressure must be the same for the three phases. The system of equations (2), whose variables are those of vector Λ (eq (1)), is the one used in this work to compute a T-3PP.

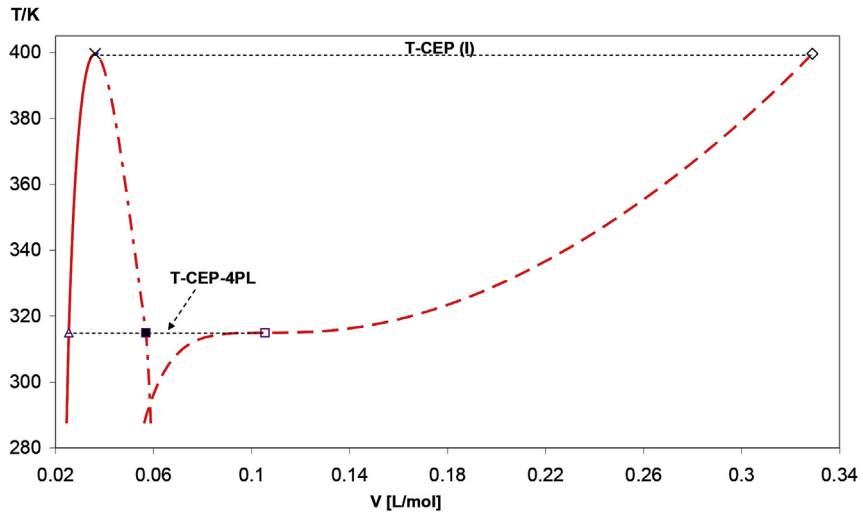

Fig. 13. Temperature-Molar Volume projection of the calculated isobaric "Special T-3PL (D)" (P = 83.36 bar = T-CEP-4PL pressure). System: *CO_2+H_2O+2-propanol* [B]. Model: SRK-EoS (see Table 4). This T-3PL is also visualized in the top part of Fig. 11. Labels: T-CEP: Ternary-critical end point. T-CEP-4PL: Ternary-critical end point of a four phase line. Phase condition associated to labels: Table 2. Important: See note in Table 4.

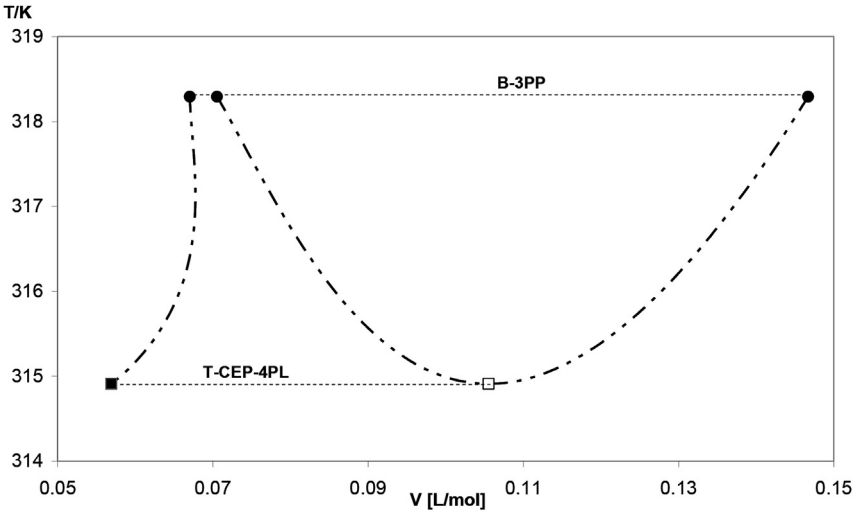

Fig. 14. Temperature-Molar Volume projection of the calculated isobaric "Special T-3PL (E)" (P = 83.36 bar = T-CEP-4PL pressure). System: *CO_2+H_2O+2-propanol* [B]. Model: SRK-EoS (see Table 4). This T-3PL is also visualized in the top part of Fig. 12. Notice that the pressure specification for this T-3PL is the same than that of Fig. 13. The B-3PP is for system CO_2+2-propanol. Labels: B-3PP: Binary three-phase point. T-CEP-4PL: Ternary-critical end point of a four phase line. Phase condition associated to labels: Table 2. Important: See note in Table 4.

Table 3
Pure compound parameters [31].

Compound	Critical Temperature (K)	Critical Pressure (bar)	Acentric Factor
2-propanol	508.3	47.64	0.6669
CO_2	304.21	73.83	0.2236
H_2O	647.13	220.55	0.3449

$$\Lambda^T = \left[T \;\; P \;\; V^\alpha \;\; V^\beta \;\; V^\gamma \;\; x_1^\alpha \;\; x_2^\alpha \;\; x_3^\alpha \;\; x_1^\beta \;\; x_2^\beta \;\; x_3^\beta \;\; x_1^\gamma \;\; x_2^\gamma \;\; x_3^\gamma \right] \tag{1}$$

$$F = \begin{bmatrix} F_1 \\ F_2 \\ F_3 \\ F_4 \\ F_5 \\ F_6 \\ F_7 \\ F_8 \\ F_9 \\ F_{10} \\ F_{11} \\ F_{12} \\ F_{13} \\ F_{14} \end{bmatrix} = \begin{bmatrix} \ln\hat{f}_1(T, V^\alpha, \mathbf{x}^\alpha) - \ln\hat{f}_1\left(T, V^\beta, \mathbf{x}^\beta\right) \\ \ln\hat{f}_1\left(T, V^\beta, \mathbf{x}^\beta\right) - \ln\hat{f}_1(T, V^\gamma, \mathbf{x}^\gamma) \\ \ln\hat{f}_2(T, V^\alpha, \mathbf{x}^\alpha) - \ln\hat{f}_2\left(T, V^\beta, \mathbf{x}^\beta\right) \\ \ln\hat{f}_2\left(T, V^\beta, \mathbf{x}^\beta\right) - \ln\hat{f}_2(T, V^\gamma, \mathbf{x}^\gamma) \\ \ln\hat{f}_3(T, V^\alpha, \mathbf{x}^\alpha) - \ln\hat{f}_3\left(T, V^\beta, \mathbf{x}^\beta\right) \\ \ln\hat{f}_3\left(T, V^\beta, \mathbf{x}^\beta\right) - \ln\hat{f}_3(T, V^\gamma, \mathbf{x}^\gamma) \\ \psi(T, V^\alpha, \mathbf{x}^\alpha) - P \\ \psi\left(T, V^\beta, \mathbf{x}^\beta\right) - P \\ \psi(T, V^\gamma, \mathbf{x}^\gamma) - P \\ x_1^\alpha + x_2^\alpha + x_3^\alpha - 1 \\ x_1^\beta + x_2^\beta + x_3^\beta - 1 \\ x_1^\gamma + x_2^\gamma + x_3^\gamma - 1 \\ h_{cut}(\Lambda) - S_{cut} \\ g_{spec}(\Lambda) - S_{spec} \end{bmatrix} = 0 \tag{2}$$

The vector Λ has 14 variables. T is the absolute temperature, P is the absolute pressure, and V^j is the molar volume of phase j. x_i^j is the mole fraction of component i in the phase j, where $i = 1..3$ and j=α, β or γ. The Greek letters α, β and γ distinguish the three phases at equilibrium. The vector F has 14 functions. The system of equations (2) is such that eqs $F_1 = 0$, $F_2 = 0$, $F_3 = 0$, $F_4 = 0$, $F_5 = 0$ and $F_6 = 0$ impose the iso-fugacity condition for all components in the three phases at equilibrium. $\hat{f}_i$ is the fugacity of component i in the mixture. Eqs $F_7 = 0$, $F_8 = 0$ and F_9=*0* impose the equal pressure condition for the three phases at equilibrium.

ψ is the function that connects explicitly the temperature (T), the molar volume (V^j) and the mole fractions x_i^j with the pressure of phase j. The mathematical forms of ψ and $\hat{f}_i$ are imposed by the selected EoS, in this work the SRK-EoS [14]. Eqs $F_{10} = 0$, $F_{11} = 0$ and $F_{12} = 0$ impose that the sum of the mole fractions of the three components must be equal to unity, for each of the three phases present.

The F_{13}=*0* and F_{14}=*0* equations are related to the two degrees of freedom that must be specified to compute a ternary three-phase equilibrium point.

The function $h_{cut}(\Lambda)$ in $F_{13} = 0$ defines the variable that is to remain constant during the computation of the T-3PL.

For example, if $h_{cut}(\Lambda) = T$ and $S_{cut} = 330\ K$, then, F_{13}=*0* becomes [T−*330 K*=*0*]. F_{13}=*0* keeps its expression invariant throughout the calculation of the T-3PL.

The $g_{spec}(\Lambda)$ function in equation F_{14}=*0* is related to the second degree of freedom that must be specified to compute a T-3PP of the T-3PL.

The function [$g_{spec}(\Lambda)$] relates to the numerical continuation method (NCM) implemented in this work [11,15]. In general, the mathematical expression of $g_{spec}(\Lambda)$ is not the same for the computation of different T-3PPs of the same T-3PL. This is dictated by the NCM.

For example, for computing a given T-3PP, the following definitions could be made: $g_{spec}(\Lambda) = V^\alpha$ and $S_{spec} = 0.1\ L/mol$. Then, F_{14}=*0* takes the form [$V^\alpha - 0.1\ \ L/mol = 0$]. This means that the NCM has decided that the most appropriate variable to be specified for this particular T-3PP is V^α, and that its value should be equal to 0.1 L/mol.

For the next T-3PP to be computed, the function $g_{spec}(\Lambda)$ could remain unmodified, or the NCM could decide to change it to, e.g., $g_{spec}(\Lambda) = P$, and to set, e.g., S_{spec}=*101.1 bar*. In such a case, the NCM would have decided that the most appropriate variable to be specified was P instead of V^α as in the previous T-3PP.

Thus, the expression for F_{14}=*0* for the next point would be [$P - 101.1\ \ bar = 0$]. The NCM uses a sensitivity analysis to identify the variable that must be specified for each point to be calculated. In addition, it determines the step length for the specified variable and predicts the values for the rest of the system variables. This ensures that the specified variable and its value, and the initial

Table 4
Interaction parameters (SRK-EOS) [14].

Ternary System	Interaction Parameters						Ref.
	k_{12}	k_{13}	k_{23}	l_{12}	l_{13}	l_{23}	
CO2(1)+H2O(2)+2-propanol(3)[A]	−0.053	0.017	−0.207	0	0	0	[21]
CO2(1)+H2O(2)+2-propanol(3)[B]	0.19	0.1215	−0.1727	0	0	0	[20]
	$1\text{-}k_{12}$	$1\text{-}k_{13}$	$1\text{-}k_{23}$				
CO2(1)+H2O(2)+2-propanol(3)[A]	1.05	0.98	1.21				
CO2(1)+H2O(2)+2-propanol(3)[B]	0.81	0.88	1.17				

Note: No attempt was made in this work to compare model predictions with experimental data. These interaction parameter values generate a highly complex phase behavior, which is enough for algorithm testing purposes and for reaching some general conclusions about the ternary fluid phase behavior.

values of the remaining variables are appropriate to obtain convergence. For more details on the NCM implemented in this work see Refs. [11,15].

A T-3PP is characterized by a number of variables (vector Λ), i.e., it is described by several coordinates, i.e., temperature, pressure, mole fractions of the components and molar volumes.

However, it is possible to add even more coordinates to a T-3PP, e.g., component fugacities, phase molar enthalpies, entropies, Gibbs energies, etcetera. Thus, (because of its several coordinates) a T-3PP is actually a hyper-point, a T-3PL a hyper-line, and a T-3PS a hyper-surface. Clearly, the prefix "hyper" means in this work "existing in more than three dimensions". Hence, a T-3PL has several possible projections in 3D space.

Two variables, chosen basically at random, out of the fourteen variables in vector Λ, can be given the status of independent variables of the T-3PP. Indeed, some restrictions apply. For instance, choosing the set of independent variables $\langle x_2^\alpha, x_3^\alpha \rangle$ is not acceptable, since eq $[x_1^\alpha + x_2^\alpha + x_3^\alpha - 1 = 0]$ becomes autonomous, and thus the system of equations (2) cannot be solved for 11 of its variables.

The allowed ranges of variation of the two independent variables define the domain of the vector function which connects such domain to the vector made of the 12 dependent variables, i.e., to the image of the vector function. A plot of a variable of the image as a function of two independent variables, is a 3D projection of a T-3PS. 2D and 3D projections are possible for T-3PLs, since a specification remains constant along a T-3PL. 2D projections are not possible for a T-3PS since the number of degrees of freedom is 2 for a T-3PS. Another ternary object that has two-degrees of freedom is a ternary critical point. Thus, the ternary critical condition gives rise to critical surfaces. Fig. 2 of ref [16] provides an example of a critical surface calculated for the system carbon dioxide + ethylene + helium, while Fig. 2 of ref [17] does the same for the systems methane + hexane + carbon dioxide and decane + hexane + carbon dioxide.

Notice that if a T-3PS is intersected by a hyper-plane where one of the system variables remains constant, e.g., the temperature, a T-3PL becomes defined. Similarly, a ternary critical surface gives rise to a ternary critical line when the surface is intersected by a hyper-plane of, e.g., constant temperature or pressure, or, e.g., constant ratio (χ) of mole fractions for two of the components of the ternary system ($\chi = x_1/x_2$). Ref. [18] presents a number of constant χ ternary critical lines, each referred to as "critical profile of a ternary mixture at a constant value of χ".

The system of equations (2) was written without specifying a particular equation of state model. Thus, it is valid for any equation of state, be it the one used here (SRK-EoS), an EoS of the SAFT family, or any other EoS.

5. Calculation of a T-3PL from a known T-4PP

The ternary three-phase behavior becomes more complex in the presence of ternary four-phase equilibrium.

Already computed ternary four-phase equilibria can be used to obtain useful information to start the calculation of T-3PLs.

At a ternary four-phase point (T-4PP), four non-critical phases coexist in equilibrium. These four phases can be identified by the labels α, β, γ, and δ. Four different combinations of three phases in equilibrium are associated to a T-4PP, i.e., α-β-γ, β-γ-δ, α-β-δ and α-γ-δ. In other words, at a T-4PP four different three-phase equilibria exist.

This implies that there are four different isothermal T-3PLs, all of them specified by identical temperature values ($T_{T\text{-}3PL(1)} = T_{T\text{-}3PL(2)} = T_{T\text{-}3PL(3)} = T_{T\text{-}3PL(4)} = T^*$), that originate at a T-4PP of equal temperature ($T_{T\text{-}4PP} = T^*$) than the one that specifies the T-3PLs. This statement is also valid for isobaric T-3PLs as long as $P_{T\text{-}3PL(1)} = P_{T\text{-}3PL(2)} = P_{T\text{-}3PL(3)} = P_{T\text{-}3PL(4)} = P_{T\text{-}4PP} = P^*$. Actually, and more generally, four T-3PLs arise from a T-44P as long $U_{T\text{-}3PL(1)} = U_{T\text{-}3PL(2)} = U_{T\text{-}3PL(3)} = U_{T\text{-}3PL(4)} = U_{T\text{-}4PP} = U^*$, where U is the temperature, or the pressure, or another 'field' variable, or combination of 'field variables' (a field variable is a variable that has the same value for every one of the phases at equilibrium). The mentioned four T-3PLs develop in different directions in the multidimensional space. This implies that four different T-3PSs meet at a T-4PL.

The specification of a T-3PL is not to be confused with that of a T-3PP: a single specification defines a T-3PL (e.g., a temperature value), while two specifications define a T-3PP.

The variables that characterize a T-4PP (similarly to a T-3PP) are: $T, P, V^\alpha, V^\beta, V^\gamma, V^\delta, x_1^\alpha, x_2^\alpha, x_3^\alpha, x_1^\beta, x_2^\beta, x_3^\beta, x_1^\gamma, x_2^\gamma, x_3^\gamma, x_1^\delta, x_2^\delta$ and x_3^δ. Unlike vector Λ in eq (1), the values for the molar volume (V^δ) and of the components mole fractions in phase δ appear for a T-4PP.

Now, assume that for a converged T-4PP the "α-β-γ" combination is chosen. Then, the values of the variables for this combination of phases will satisfy the system of equations (2). In this way, the T-4PP provides a 'converged' T-3PP for the "α-β-γ" combination.

From this converged T-3PP it is possible to start building an associated (properly specified) complete T-3PL using the numerical continuation method.

Note that each of the four three-phase combinations is a mathematically converged T-3PP (under the T-4PP conditions of such combination).

However, even though the T-3PP is a converged point, the direction in which the calculation of an associated T-3PL must progress is yet to be determined.

For example, along the T-3PL, the temperature of a T-3PP located very close to the T-3PP coincident with the T-4PP, could be either greater than the T-4PP temperature, or less than the T-4PP temperature. Nevertheless, there is only one direction in which the T-3PL is thermodynamically stable. The right direction along which the T-3PL develops is not known in advance.

To determine the direction along which the T-3PL is stable, a stability test is applied to the second (already computed) point of the T-3PL. If such point is stable, then, the calculation proceeds in

the direction indicated by such point (e.g., in a direction of increasing temperature), otherwise, it is made to proceed in the opposite direction (e.g.: in a direction of decreasing temperature). The stability test applied in this work is described in general terms in Ref. [19].

Appendix A describes ways of obtaining a first converged point for T-3PLs which originate at equilibrium points which are not T-4PPs.

6. Results

In order to study the complexities of the ternary three-phase equilibrium behavior, a variety of T-3PLs for the *CO_2(1)+H_2O(2)+2-propanol(3)* system were computed.

This system was selected due to the asymmetry between its components, which results in more complex behaviors, including the phenomenon of ternary equilibrium among four fluid phases.

As previously stated, the computed phase behavior for a given system depends on the chosen equation of state and on the values of pure compound and interaction parameters used in the calculations. In this work the SRK-EoS [14], coupled to van der Waals quadratic mixing rules, was used to perform the calculations. Two different sets of interaction parameters (Table 4) were used to compute T-CMs and a variety of T-3PLs. The interaction parameters were taken from the literature [20,21]. No attempt was made in this work to compare the model predictions with experimental data, such as data on three-phase equilibria of the component binary sub-systems, or data on ternary four-phase equilibria. The choice of the SRK-EoS is acceptable, in spite of the relative simplicity of the pressure-temperature-density-composition relationship that it sets. This is because such EoS is capable of capturing, at least at qualitative level, phenomena of great complexity, e.g., the multiplicity of T-3PSs in ternary systems. Such capability is all we need for performing the task of subjecting the calculation algorithms (of general applicability here proposed) to stringent enough tests.

The SRK-EoS is not a state-of-the-art EOS, while more modern molecularly based EoSs of the SAFT family are. SAFT-type EoSs are significantly more complex, in their mathematical forms, than the simple SRK-EoS, giving rise to problems such as the existence of multiple molar volume roots [22]. This may imply the prediction of a liquid–liquid–vapour (LLV) triple point for a pure compound [22], which is, already at qualitative level, nonrealistic. This behavior, which is not acceptable, was found for a large number of chemicals [22]. If the chosen model predicts the existence of a pure compound LLV point, for one of the components of a binary system, then, it will also predict the existence of a binary LLV line originating at such triple point. In principle, such kind of binary LLV line has never been experimentally observed. In turn, this binary LLV line will be, if a third component is added, a boundary line of a predicted (indeed spurious) T-3PS that could eventually extend towards high temperatures and pressures. Under such circumstances, the molecularly based nature of the model might not be of enough help in generating valuable insights into the underlying causes of three-phase equilibria in ternary mixtures. Beyond these remarks on older and newer EoSs, it is not the purpose of this work to advocate or criticize particular EoSs. Otherwise, it is to test algorithms (which are applicable to any EoS-type model) in challenging situations; and also to properly interpret the results that they generate. See Refs. [23–27] to explore the wide variety of available EOSs, and to find out about their strengths and limitations, and about challenges to be faced in their future development.

It is worth noting the exceptional behavior of helium, which does have a fluid-fluid-fluid triple point, i.e., a helium I/helium II/gas triple point. Helium I is a normal liquid and helium II a superfluid (see page 391 of ref [28]).

Actually, the parameters in Ref. [20] do not correspond to the SRK-EOS but to a similar model, i.e., to the Peng-Robinson EOS. This is not a problem since the focus of this work is the study of the possibilities for the three-phase ternary behavior, and not the evaluation of the quantitative performance of the model. This approach is essentially the same that the one used in Ref. [3] for binary systems. Ref. [3] was a contribution of significant importance for the identification of the main patterns of the binary phase behavior.

To distinguish between the two different sets of parameters, the labels/terms "*CO_2(1)+H_2O(2)+2-propanol(3)* [A]" system (or system [A]) and "*CO_2(1)+H_2O(2)+2-propanol*(3) [B]" system (or system [B]) are used.

Table 3 shows the values for critical temperature (Tc), critical pressure (Pc) and acentric factor (w) for the pure components. The numerical values of each set of interaction parameters are shown in Table 4. Table 5 shows the types of phase behavior (types of B-CMs) obtained for each binary sub-system, according to the classification in Ref. [3]. These behaviors were identified in this work through the use of the calculation algorithms described in Ref. [4]. Each set of parameters results in a qualitatively different behavior of the T-CM and, consequently, of the computed T-3PLs.

Section 6.1 shows results for system [A]. Such results, among other outcomes, confirm the reliability of the calculation procedures proposed in section 5 and in Appendix A. Section 6.2 focuses on the relationship among T-3PSs and T-4PLs through the study of computation results obtained for system [B].

6.1. Phase behavior of the ternary system [A]

In this section, the system [A] (Table 4) is used in testing the calculation procedures proposed in section 5 and Appendix A. 2D and 3D projections of a number of T-3PLs are shown.

Figs. 2–4 show the extent and endpoints of the T-3PLs (I), (II), (III), (IV), (V) and (VI), in the pressure-temperature plane, together with computed univariant lines of the T-CM of system [A].

The mentioned T-3PLs are straight lines in the PT plane, because their calculation was performed at constant temperature, or at constant pressure, or maintaining a non-isobaric non-isothermal linear relationship between P and T.

Figs. 2–4 do not provide information about the topology of the T-3PLs in the multi-dimensional space, but are useful to illustrate the variety of bounds between which the T-3PLs exist.

The T-CM of Fig. 2 for system [A] is the same than that of Fig. 1. The endpoints indicated for the T-3PLs in Fig. 2 help in inferring what the possible limits are for the T-3PSs.

It is important to remember that the T-3PLs and the T-3PSs are not thermodynamic objects of the T-CM: but the boundaries of the T-3PSs are (e.g., the T-CELs). The isobaric T-3PL (II) (Fig. 2) begins in a B-3PP of the B-3PL (CO_2+H_2O) and ends in a T-CEP of the T-CEL(e).

The also isobaric T-3PL (IV) (Fig. 2) begins in a B-CEP (CO_2+H_2O) (Fig. 2, empty circle) and ends in a T-CEP of the T-CEL(e). The procedures described in Appendix A in sections A.1 and A.3, were used to compute the T-3PLs (II) and (IV) (Fig. 2) respectively.

Table 5
Types of phase behavior of the binary sub-systems.[a]

Ternary System	Type of binary behavior [3]		
	1–2	1–3	2–3
CO_2(1)+H_2O(2)+2-propanol(3)[A]	III	II	I
CO_2(1)+H_2O(2)+2-propanol(3)[B]	III	III	II

Model: SRK-EoS [14]. Parameters from Tables 3 and 4.
[a] Obtained from computed binary univariant lines.

Fig. 3 (zoom of Fig. 2), shows the isobaric T-3PLs (I) and (V).

The calculation of the T-3PL (I) (Fig. 3) began in a T-4PP of the T-4PL and ended in a T-CEP of the T-CEL (c) (Fig. 3). On the other hand, the computation of T-3PL (V) (Fig. 3) started off at the T-CEP-4PL and also ended in a T-CEP of the T-CEL(c) (Fig. 3).

The isothermal T-3PL (III) shown in Fig. 3, develops between two T-CEPs, one of the T-CEL (b) and the other of the T-CEL (c). The calculation of the T-3PL (I) has been described in section 5; of the T-3PL (III) in Appendix A, section A.2; and of the T-3PL (V) in Appendix A, section A.4.

In order to illustrate the phenomena that takes place close to the T-TCP when a continuous set of three-phase equilibria approaches such point, a linear relationship between pressure and temperature (which are both 'field' variables) was established to compute the T-3PL (VI) shown in Fig. 4. T-3PL (VI) begins in a T-4PP and ends at the T-TCP (II) (=T-TCEP(II)).

The linear relationship $(P-(aT+b)=0)$, where a=(1.8841 bar/K) and b=(-519.04 bar), was established as equation $F_{13}=0$ in the system of equations (2) of section 4, to specify the T-3PL (VI) of Fig. 4. A linear relationship between P and T, used to specify a T-3PL, can be set in a laboratory equilibrium study if a variable volume cell and a thermostat are available.

A procedure to start off the calculation of a T-3PL from a known T-TCP has not yet been developed (see Appendix A, section A.5).

Figs. 5–7 show projections for the calculated T-3PLs (III) and (IV) involving the phase molar volumes or the phase compositions. The labels L1, L2 and L3 identify the phases at equilibrium in the different T-3PLs.

Fig. 5 shows the pressure-molar volume projection of the isothermal T-3PL (III). Fig. 5 makes possible to read the molar volumes of each of the phases at equilibrium at a specified pressure.

In this projection, the critical phenomenon can be clearly appreciated when the T-3PL(III) reaches the T-CEP (b) or the T-CEP(c).

The molar volumes of the phases L1 and L2 tend to be equal as the three phases at equilibrium approach the T-CEP(c) at low pressure, i.e., both phases become critical at the T-CEP(c) (L1 = L2, Fig. 5).

Similarly, the molar volumes of the phases L2 and L3 become equal, and such phases become critical, when the T-3PL(III) reaches the T-CEP (b) at high pressure (L2 = L3, Fig. 5).

Fig. 6 shows the T-3PL (IV), which has a B-CEP as its endpoint at low temperature, for which the critical phases are L2 and L3(=L2). Note that this T-3PL begins at a point of a binary system (CO_2+H_2O) where, actually, 2-propanol is at infinity dilution. When the T-3PL (IV) in Fig. 6 reaches the T-CEP (e) the critical phases are L1 and L2(=L1). The curve labeled L2 in Fig. 6 does not seem to be smooth enough in the region around a temperature value of about 315 K. This perception arises from the fact that Fig. 6 is just a 2D projection of the multidimensional T-3PL(IV). We have verified that 3D projections of the T-3PL(IV), whose variables are the temperature, the molar volume of phase L2, and some other variable such as the mole fraction of CO_2 in phase L2, show curves that are clearly smooth along the whole range of existence of the T-3PL(IV), as are the curves shown in Fig. 7 for the same T-3PL. In other words, the apparent lack of sufficient smoothness for curve L2 in Fig. 6 is spurious. In general terms, 2D projections of smooth multidimensional curves can even show discontinuities in their slopes.

Another type of projection of T-3PL(IV) is shown in Fig. 7.

The base of the prism is the Gibbs triangle where phase compositions are represented. The vertical axis is the temperature. The concentration scale is the mole fraction.

The (horizontal) triangle inside the prism with vertices L1, L2 and L3 is a T-3PP, at set pressure and temperature, and the segments L1-L2, L1-L3 and L2-L3 are the corresponding tie lines. Other (horizontal) T-3PPs are indicated in Fig. 7.

The region enclosed by the tie-lines, is the region where the three-phase equilibrium exists for a given pressure and temperature. Any overall composition of the ternary system (for a specified temperature and pressure) within this region will produce three phases at equilibrium (L1+L2+L3), where the composition of each phase is given by the vertices of the three-phase triangle.

The end points in Fig. 7 are indeed the same than those in Fig. 6 [B-CEP(CO_2+H_2O) and T-CEP(e)].

Fig. 7 clearly shows that the B-CEP of the T-3PL(IV) is on the (CO_2+H_2O) side (vertical prism face). In the low temperature end (B-CEP) of the T-3PL(IV) the length of the L2-L3 side tends to zero. The same is true for the L1-L2 side in the high temperature end (T-CEP(e)).

In Appendix B, the temperature-molar volume projections for T-3PLs (I), (II), (V) and (VI) are shown.

Ternary two-phase equilibria can also be represented in Gibbs prisms as the one shown in Fig. 7. These equilibria have three degrees of freedom, and their representation in Gibbs prisms is possible only after having spent one of them, e.g., by setting the pressure value (as it has been done in Fig. 7, where pressure equals 76.17 bar). A continuous set of ternary two-phase equilibria at set pressure (or set temperature) would be seen, in a Gibbs prism, as a surface or as a couple of surfaces, depending on the presence or absence of a critical line. However, in general terms, the geometrical object associated to an unrestricted continuous set of ternary two-phase equilibria is not a surface (or hyper-surface, which only has two degrees of freedom) but another geometrical object that has three degrees of freedom. Such geometrical object has no projections in the 3D space. These require that the number of degrees of freedom be less than or equal to two. Ternary two-phase equilibria at set temperature, represented in a Gibbs prism, can be seen in, e.g., fig C.1. of Ref. [11]. Fig. 5 in Ref. [29] is another example of calculated two-phase and three-phase equilibria represented in a Gibbs prism. Such figure was obtained for the system carbon dioxide-benzene-water at 14.2 MPa in a wide temperature range [29].

6.2. Phase behavior of the ternary system [B]

In this section, the system [B] (Table 4) is used to analyze the relationship among the ternary four-phase equilibria and the T-3PSs.

Fig. 8, shows the computed univariant lines and invariant points for the pure components, for the binary sub-systems and for the ternary system [B]. Fig. 8 is the complete T-CM for the system [B].

From the B-CEP (H_2O+*2-propanol*) (highest temperature empty circle in Fig. 8), the T-CEL(I) begins, and ends at a T-TCP. From this T-TCP the T-CEL (II) begins and extends towards high pressures (Fig. 8).

Fig. 9 (zoom Fig. 8), shows in its top left insert (Zoom B) the T-CEL (III) which begins at the B-CEP (CO_2+H_2O) and ends at a T-CEP-4PL (empty triangle), at which the T-CEL (IV) originates. This line ends at the B-CEP (CO_2+*2-propanol*, Fig. 9). Finally, from the T-CEP-4PL the T-4PL begins and extends towards low pressures and temperatures.

The existence of B-3PLs, T-CELs and T-4PLs in Figs. 8 and 9 imply that three-phase equilibria exist for system [B]. Besides, the presence of the T-4PL indicates that there are four different T-3PSs that originate at this line. The phases at equilibrium in the T-4PL are distinguished by the labels "α-β-ω-ε" where each Greek letter represents one of the phases at equilibrium. To outline the topology of each of the four T-3PSs, different sets of T-3PLs were computed. To distinguish among the four T-3PSs the labels (1), (2), (3) and (4) are used. Figs. 10–12 show P-T-$\ln(\hat{f}_1)$ projections for the T-3PSs (1),

(2), (3) and (4) (green labels). $\hat{f}_1$ is the fugacity for the component 1 (CO_2 in this case) in the ternary heterogeneous system at equilibrium. The advantage of selecting the variable $\hat{f}_1$, in Figs. 10–12, is that it has the same value in each of the equilibrium phases (i.e., the component fugacity is a field variable, as are T and P). The use of the three field variables P, T and $\ln(\hat{f}_1)$ makes possible to visualize more easily the T-3PSs and their boundaries.

To fix ideas, notice that, e.g., Fig. 10, makes possible to read, e.g., the value of the fugacity of CO_2, at set temperature and pressure, when CO_2 participates in a three-phase equilibrium together with water and 2-propanol. In the process of reading such fugacity, the two degrees of freedom associated to the ternary three-phase equilibrium (T and P) are set.

Fig. 10 shows the T-3PS (1), which is outlined by the shown "set 1" (S1) and "set 2" (S2) of isothermal and isobaric T-3PLs (red lines indicated by arrows). The phase combination of the T-3PS (1) is: α-ω-ε. The S1 T-3PLs are isothermal and the S2 T-3PLs are isobaric. The boundary of T-3PS (1) [S1+S2] is made of the T-CEL (I), the T-TCP, the T-CEL(II), the T-4PL, and the T-CEP-4PL.

The sets of T-3PLs "set 3" (S3) and "set 6" (S6) (Fig. 11) outline the T-3PS (2). The phase combination of the T-3PS (2) is: α-β-ω. The S3 T-3PLs (Fig. 11) are isobaric and the S6 T-3PLs are isothermal. The T-3PS (2) [S3+S6] can be appreciated in Fig. 11. The boundary of T-3PS (2) [S3+S6] is made of the B-3PL (*H_2O+2-propanol*), the B-CEP (*H_2O+2-propanol*), the T-CEL(I), the T-4PL, and the T-CEP-4PL.

Note that the B-3PL (*H_2O(2)+2-propanol(3)*), to which the "B-3PPs" indicated in Figs. 10 and 11 belong, cannot strictly be shown in a diagram (such as Figs. 10 and 11) having as one of its variables the $\ln(\hat{f}_1)$, i.e., the variable $\ln(\hat{f}_{CO_2})$. When a T-3PL tends to a point of the B-3PL(*H_2O+2-propanol*), the concentration of CO_2 tends to zero, so does $\hat{f}_{CO_2}$, and $\ln(\hat{f}_{CO_2})$ tends to minus infinity. In Figs. 10 and 11, the "red empty circles" are strictly T-3PPs (strictly not B-3PPs), but they are located very close to the B-3PL (*H_2O+2-propanol*), due to their very low CO_2 concentration. In the same way, the "blue empty circle" in Figs. 10 and 11 is strictly a T-CEP (strictly not a B-CEP) located however very close to the B-CEP (*H_2O+2-propanol*), at which the T-CEL (I) originates.

The isothermal T-3PL (B) and T-3PL (C) indicated in Figs. 10 and 11 were computed at the same temperature. Both are located within the same vertical plane. Hence, both lines meet the same point (T-4PP) of the T-4PL in the projection of Figs. 10 and 11. The T-3PL (B) is located above the T-4PL while the T-3PL (C) is below it (Fig. 11).

For a point on the T-3PL(B) at a pressure infinitesimally greater than the T-4PP pressure, the phases are α-ω-ε (Fig. 11). On the other hand, for a point of the T-3PL(C) at a pressure infinitesimally below the T-4PP pressure the phases are α-β-ω (Fig. 11). In this case, there is an evident change in the type of one of the phases at three-phase equilibrium when crossing the T-4PL. We would thus state that the T-4PL separates the T-3PS(1) from the T-3PS(2).

Let us focus now on the isothermal high-temperature (special) T-3PL (A) [T = 348.38 K] shown in Fig. 10. This T-3PL is located within a vertical plane and originates at a point on the T-CEL (II), and ends at a B-3PP (*H_2O+2-propanol*). At high pressure, i.e., close to the T-CEP(II) at 348.38 K, the phases of the T-3PL (A) are α-ω-ε. This combination of phases corresponds to the T-3PS (1). In contrast, at low pressure, close to the B-3PP at 348.38 K, the phases of the T-3PL (A) are α-β-ω, and this combination corresponds to the T-3PS (2). Thus, in T-3PL (A), the ε phase present at high pressure evolved, through a continuous transition, into phase β.

We now revise our previous statement and say that the T-4PL does not separate completely the T-3PS (1) from the T-3PS (2). Fig. 11 shows that it is possible to draw a relatively arbitrary, but continuous, path, on the T-3PSs, for going from point (A) of the T-3PS(2) to point (B) of the T-3PS(1) without ever crossing the T-4PL, which implies that a continuous transition between phases β and ε occurs. This is an interesting outcome that could be visualized because only field variables were considered in the projection of Figs. 10 and 11.

Fig. 12 shows the T-3PSs (3) and (4).

The boundary of the T-3PS (3) is made of the B-3PL (CO_2+H_2O), the B-CEP (CO_2+H_2O), the T-CEL(III), the T-CEP-4PL and the T-4PL. This surface is outlined by the "set 4" (S4) of T-3PLs, where some of the T-3PLs were computed at constant temperature and some of them at constant pressure.

The phase combination that characterizes the T-3PS (3) is β-ω-ε.

The boundary of T-3PS (4) is made of the B-3PL (CO_2+*2-propanol*), the B-CEP (CO_2+*2-propanol*) the T-CEL(IV), the T-CEP-4PL and the T-4PL. This surface is outlined by the "set 5" (S5) of T-3PLs, again with some T-3PLs computed at constant temperature and some at constant pressure.

The phase combination that characterizes the T-3PS (4) is α-β-ε.

It is not possible to draw a continuous path in Fig. 12 connecting a T-3PP of the T-3PS (3) to a T-3PP of the T-3PS (4) without meeting the T-4PL. Thus, there is no continuous transition between T-3PS (3) and T-3PS (4).

The T-4PL, as previously stated, extends indefinitely towards low temperatures and pressures. Consequently, the same is true for the T-3PSs (1), (2), (3) and (4), i.e., these surfaces have no definite low temperature – low pressure limit. This is because the T-4PL is a boundary common to all four T-3PSs, or, in other words, any of the T-3PSs has the T-4PL as one of its boundaries.

Table 6 summarizes the boundary constitution for each of the four T-3PSs.

We stress that, as Fig. 11 shows, at a temperature T less than the T-CEP-4PL temperature ($=T^{\oplus}$), i.e., at $T < T^{\oplus}$, the T-3PSs (1) and (2) provide a couple of isothermal T-3PLs (a T-3PL each), while at $T > T^{\oplus}$ they provide a single isothermal T-3PL. The transition from two to one T-3PLs happens at $T = T^{\oplus}$. Thus, when considering only the T-3PSs (1) and (2) of Fig. 11, we conclude that only a single isothermal T-3PL contains the T-CEP-4PL, or, vice versa, that a single isothermal T-3PL originates at such point, with the particular feature of being stable at either side of the T-CEP-4PL. Notice that the T-CELs of the T-3PSs (1) and (2) (i.e., T-CEL(I) and T-CEL(II), Figs. 10 and 11) do not contain the T-CEP-4PL.

The previous statements are also valid for isobaric T-3PLs, i.e., when considering only the T-3PSs (1) and (2) (Fig. 10), a single isobaric T-3PL originates at the T-CEP-4PL and it is stable both at higher and at lower temperatures than $T^{\oplus}$. Such isobaric line is

Table 6
Description of the four T-3PSs originating at the T-4PL for system [B].[a]

T-3PS	Combination of phases from the T-4PL that give rise to the T-3PS	Constitution of boundary[b]
T-3PS (1) (Figs. 10 and 11)	α-ω-ε	T-CEL (I), T-TCP, T-CEL(II), T-4PL and T-CEP-4PL
T-3PS (2) (Figs. 10 and 11)	α-β-ω	B-3PL (*H_2O+2-propanol*), B-CEP (*H_2O+2-propanol*), T-CEL(I), T-4PL and T-CEP-4PL
T-3PS (3) (Fig. 12)	β-ω-ε	B-3PL (CO_2+H_2O), B-CEP (CO_2+H_2O), T-CEL(III), T-CEP-4PL and T-4PL
T-3PS (4) (Fig. 12)	α-β-ε	B-3PL (CO_2+*2-propanol*), B-CEP (CO_2+*2-propanol*), T-CEL(IV), T-CEP-4PL and T-4PL

[a] See Table 4.
[b] All T-3PSs have no definite low pressure low temperature boundaries.

indicated as "Special T-3PL (D)" in Fig. 11, and it is shown in Fig. 13. There we see that no pair of phases become identical at the T-CEP-4PL, which could be regarded as curious or even surprising. Actually, such behavior would also be seen in, e.g., a binary two-phase equilibrium isotherm (Pxy diagram) of temperature equal to that of a B-CEP; or, e.g., in a continuous set of ternary two-phase equilibria at set *T* and *P*, if, e.g., the pressure *P* is set equal to that of a T-CEP at the set *T*.

The critical phase of the T-CEP-4PL in Fig. 13 is the one with highest molar volume (empty square in Fig. 13). Although no pair of phases is such that both phases become identical at the temperature of the T-CEP-4PL, it is seen in Fig. 13 that the dashed branch becomes extremely flat when the branch-phase becomes critical (empty square). The flatness of curves involving a phase molar volume and a field variable such as T (as in Fig. 13 dashed line) is a behavior seen in other contexts, e.g., for the critical isobar (T vs molar volume, P=Pc) at V=Vc for a pure compound; or for the experimental T vs molar volume vapour-liquid equilibrium hypercurve, at V=Vc for a pure compound. Notice that the intersection point (in Fig. 13) between the dashed branch and the dashed-dotted branch, which happens at a pressure (about 290 bar) less than the T-CEP-4PL pressure in Fig. 13, is not a critical point. An experimentalist following the T-3PL of Fig. 13 in a visual cell when going, e.g., from lower to higher temperatures, would not notice passing through the T-CEP-4PL, this being said in the sense that he/she would not see the appearance or disappearance of a phase at such point, or a change in the number of phases. What it would probably be seen is the critical opalescence of the phase indicated with the empty square in Fig. 13, when passing through the T-CEP-4PL. There is a second instance where a critical state is met by the T-3PL in Fig. 13. This happens at the highest temperature in Fig. 13, where the two phases which were not critical at the T-CEP-4PL (empty triangle and full square) become critical (cross (×), label T-CEP(I) in Fig. 13).

On the other hand, from looking at Fig. 12 (or at Fig. 9), corresponding to the T-3PSs (3) and (4), at $T < T^{\oplus}$ two isothermal T-3PLs exist, while at $T > T^{\oplus}$ a single isothermal T-3PL exists, which is contributed by the T-3PS (4). Again, the transition between these two behaviors takes place at $T = T^{\oplus}$, where the T-3PS (4) provides a single T-3PL that contains the T-CEP-4PL. The T-CELs of the T-3PSs (3) and (4) (i.e, T-CELs (III) and (IV)) do contain the T-CEP-4PL (Fig. 9).

In conclusion, if the specification $T = T^{\oplus}$ is made, with the aim of computing, at such temperature, all the T-3PLs related to the T-4PL, then, each couple of T-3PSs contributes, for the case of system [B], with a single T-3PL. In other words, only two isothermal T-3PLs stem from a T-CEP-4PL for system B. This conclusion (i.e., maximum number of T-3PLs equal to two) should be valid, for system [B], also for specifications involving other field variables, or combinations of them.

For system [B], the second isobaric T-3PL of pressure equal to that of the T-CEP-4PL (P = 83.36 bar), is shown in Fig. 14. This T-3PL is identified in Fig. 12 as "Special T-3PL (E)".

This T-3PL (Fig. 14) originates at a B-3PP(CO_2+2-propanol) and ends at the T-CEP-4PL of which only two phases (out of three) are shown in Fig. 14. The qualitative behavior at the T-CEP-4PL is for the T-3PL(E) in Fig. 14 clearly different from that of T-3PL(D) in Fig. 13. This is more easily seen in Fig. 15: while two phases become identical at the T-CEP-4PL temperature for T-3PL(E) (black branches), no pair of phases do so for the T-3PL(D) (red branches). At a given temperature, say, at 317 K, in Fig. 15, there is a range of overall composition of the ternary system compatible with one (black) of the two possible three-phase sets, and a different range (which does not overlap with the previous one) compatible with the other (red) three-phase set.

The phase behavior in Fig. 8 is significantly different from that of Fig. 2, i.e., the impact of the changes (shown in Table 4) in the interaction parameters on the phase behavior of the ternary system is very important. The attractive energy parameter of the SRK-EOS, when used coupled to quadratic mixing rules, is proportional to the factors $(1\text{-}k_{ij})$. We remind that $k_{ii} = 0$ and that $k_{ij} = k_{ji}$ (symmetric crossed interaction parameters), and that all $(1\text{-}k_{ij})$ factors should in principle be greater than zero, regardless the sign of k_{ij}. The actual restriction is that the mixture attractive energy parameter has to be positive at all temperatures and system compositions, which is met, in particular, by setting $(1\text{-}k_{ij})$ greater than zero. At constant composition and temperature, an increase in the factor $(1\text{-}k_{ij})$ makes the attractive energy parameter of the mixture increase. The values of the $(1\text{-}k_{ij})$ factors are presented in Table 4 for systems [A] and [B]. All three values of $(1\text{-}k_{ij})$ are greater for system [A], i.e., system [A] is more attractive than system [B] (bear in mind that all pure compound parameters are the same for both systems). For the SRK-EOS, a higher attractive energy parameter implies, in general, a higher tendency to liquid homogeneity or "affinity" [30]. Thus, due

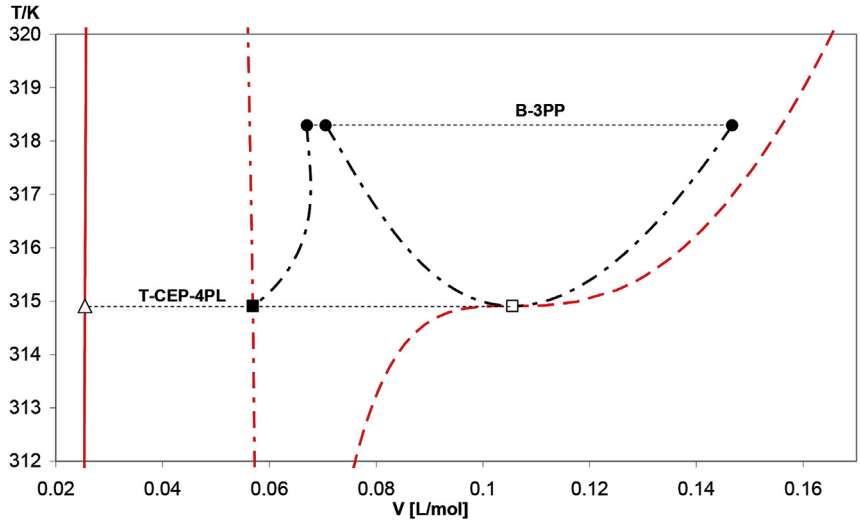

Fig. 15. Phase equilibria of Figs. 13 and 14 shown together. Labels: B-3PP: Binary three-phase point. T-CEP-4PL: Ternary-critical end point of a four phase line. Phase condition associated to labels: Table 2. Important: See note in Table 4.

to its higher affinity, system [A] should have less tendency to three-phase equilibria than system [B], i.e., the size in the PT plane of the three-phase equilibrium region should be less for system A, when compared to system B. This can be verified from comparing Fig. 2 with the set of Figs. 8 and 10.

In Fig. 2 (system [A], higher affinity), the ternary three-phase equilibria is confined, in the PT plane, to the region in between the T-CEL(e) and lines: B-3PL(CO_2+H_2O), T-CEL(a) and T-CEL(d). In Fig. 8, such equilibria is basically found to the left of T-CEL(I) and T-CEL(II), with no lower limit in temperature and no upper limit in pressure. Clearly, in the temperature range of Fig. 2, system [A] (higher affinity) has ternary three-phase equilibria in a significantly smaller region than system [B] (lower affinity, Figs. 8 and 10). Actually, from computation results not shown here, system A presents ternary three-phase equilibria also at low temperatures, outside the temperature range of Fig. 2, such that, at high enough pressure, such equilibria happens in narrow ranges of temperature. Thus, at low temperature, system B (Fig. 10) still has more tendency to three-phase equilibria than system A.

To fix ideas even further, notice that the binary *H_2O(2)+2-propanol(3)* is of type II (Table 5, last column, system [B]) for (1-k_{23}) = 1.17 (Table 4, system [B]) and type I for (1-k_{23}) = 1.21. Type II systems have binary three-phase equilibrium, while Type I systems do not. In other words, when increasing the affinity level from 1.17 to 1.21 the three-phase equilibrium disappears.

The B-CEP of system CO2(1)+2-propanol(3) is located at about 327 K for system [B] (Fig. 9), and (from calculation results not shown here) at about 86 K for system [A]. Since the B-CEP is the endpoint of the B-3PL, it should be clear that when the affinity level increases from (1-k_{13}) = 0.88 (system [B], Table 4) to (1-k_{13}) = 0.98 (system [A], Table 4) the termination of the binary three-phase equilibrium is moved to much lower temperatures, over a distance in the order of 200 K (from 327 K to 86 K). Notice that binary liquid immiscibility for systems of type II and III (Table 5, "1–3" column) is not possible at temperatures greater than the B-CEP temperature.

The location of the CO2(1)+ H_2O(2) B-3PL is similar for systems [A] and [B] (Fig. 1, insert in right bottom corner; Fig. 9, insert in top left corner). However, the critical line that originates at the pure H_2O critical point is significantly different for such systems. In Fig. 8 (system [B]), it can be seen that the critical temperature value found in the B-CL (*CO_2(1)+H_2O(2)*) at 600 bar is about 600 K. If pressure is increased to 1936 bar, the calculated critical temperature becomes approximately equal to 597 K. On the other hand, the same binary system, but with parameters corresponding to system [A] (Table 4) has, at 1939 bar, a calculated critical temperature of only 486 K. In other words, when the pressure is in the order of 1940 bar, the critical temperature of system CO_2+H_2O is reduced by about 110 K (from 597 K to 486) when going from system [B] to system [A], i.e, when going from (1-k_{12}) = 0.81 to (1-k_{12}) = 1.05. The reduction of the critical temperature at such high pressure indicates an increase in liquid miscibility, i.e., an increase in affinity, due in this case to the increase in the attractive energy parameter of the binary system.

7. Remarks and conclusion

The calculation procedures developed in this work for computing different types of ternary three-phase equilibrium lines (T-3PLs) were found to be efficient and free from convergence problems.

Such procedures are described in section 5 and in Appendix A. They take advantage of the information contained in (previously computed) phase equilibrium objects which contribute to the boundaries of the ternary three-phase surfaces (T-3PSs). Such information is used to start off the calculation of the T-3PLs. The mentioned objects are invariant points of the ternary fluid phase equilibrium characteristic map (T-CM), or points of univariant lines of such map; and they act as termination/originating points of the T-3PLs. The absence of convergence problems during the building of the T-3PLs is due to the use of a numerical continuation method (NCM). The NCM makes possible to compute a complete T-3PL in a single run. The couple of ternary model systems studied are highly asymmetric. The computation of their phase behavior is a stringent test for any proposed calculation algorithm.

A large enough number of computed T-3PLs makes possible to visualize the topology of T-3PSs (e.g. Fig. 11), if 3D projections involving only field variables are used. Computation results show that there can be continuous transitions between T-3PSs. This in turn implies the existence of special T-3PLs having a point for which one of the phases reaches a critical condition but without becoming identical to any of the other two phases (Fig. 13). This may be considered to be surprising or unexpected.

A thorough account of the possible constitutive elements of the boundaries of T-3PSs seems not to have been available in the open literature up to now. This work fills such void.

The knowledge of the potential variety of the ternary three-phase equilibrium that can be unveiled through computations as those of the present work, should be helpful in the interpretation of measurements carried out in the laboratory.

The changes found in the ranges of conditions, where the computed ternary three-phase equilibrium takes place, are explained in this work in terms of changes in the attractive energy parameter of the system.

Acknowledgments

We gratefully acknowledge the financial support from the Argentinean institutions: Consejo Nacional de Investigaciones Científicas y Técnicas (CONICET, grant ID: PIP 11220150100918), Agencia Nacional de Promoción Científica y Tecnológica (ANPCyT, grant ID: PICT-2012-1998) and Universidad Nacional del Sur (UNS, grant ID: PGI 24/M148).

Appendix A. Techniques for starting off the computation of T-3PLs from known B-3PPs, T-CEPs, B-CEPs and T-CEPs-4PL

A.1-Starting off from a B-3PP to which the T-3PL tends

From section 4, the variables that characterize a T-3PP are T, P, V^{α}, V^{β}, V^{γ}, x_1^{α}, x_2^{α}, x_3^{α}, x_1^{β}, x_2^{β}, x_3^{β}, x_1^{γ}, x_2^{γ} and x_3^{γ}. In a B-3PP the mole fraction variables x_3^{α}, x_3^{β} and x_3^{γ} (which imply the presence of the third component in each of the three phases) do not exist. A known converged B-3PP is useful to obtain a T-3PP where the third component is practically at infinity dilution while the other components have concentrations practically equal to those of the B-3PP.

More specifically, the procedure to initialize the variables of this T-3PP is to set T, P, V^{α}, V^{β}, V^{γ}, x_1^{α}, x_2^{α}, x_1^{β}, x_2^{β}, x_1^{γ}, x_2^{γ} equal to those of the known B-3PP, while x_3^{α}, x_3^{β} and x_3^{γ} are initialized to a value such that component 3 is highly diluted, for example at a mole fraction value equal to 1×10^{-6}. If convergence is not achieved, then, only one of the three mole fractions of the third component is set equal to a value in the order of 1×10^{-6}, e.g., $x_{3,\infty}^{\alpha} = 1 \times 10^{-6}$. The subscript "$\infty$" indicates "close to infinite dilution". Subsequently, the mole fractions of the component "3" in phase "β" and in phase "γ" are estimated using the following equations:

$$x_{3,\infty}^{\beta} = \frac{\widehat{\varphi}_3^{\alpha}\left(T, V^{\alpha}, x_1^{\alpha}, x_2^{\alpha}, x_{3\to 0}^{\alpha}\right)}{\widehat{\varphi}_3^{\beta}\left(T, V^{\beta}, x_1^{\beta}, x_2^{\beta}, x_{3\to 0}^{\beta}\right)} \cdot x_{3,\infty}^{\alpha} \tag{A.1.1}$$

$$x_{3,\infty}^{\gamma} = \frac{\widehat{\varphi}_3^{\alpha}\left(T, V^{\alpha}, x_1^{\alpha}, x_2^{\alpha}, x_{3\to 0}^{\alpha}\right)}{\widehat{\varphi}_3^{\gamma}\left(T, V^{\gamma}, x_1^{\gamma}, x_2^{\gamma}, x_{3\to 0}^{\gamma}\right)} \cdot x_{3,\infty}^{\alpha} \tag{A.1.2}$$

where $x_{3,\infty}^{\beta}$ and $x_{3,\infty}^{\gamma}$ are the mole fractions of component "3" in the "β" and "γ" phases respectively, while $\widehat{\varphi}_3^{\alpha}$, $\widehat{\varphi}_3^{\beta}$ and $\widehat{\varphi}_3^{\gamma}$ are the fugacity coefficients of component 3 in the phases α, β and γ respectively. The fugacity coefficients are evaluated under the condition that the mole fraction of component 3 tends to zero in each of the phases. This is expressed as $x_{3\to 0}^{\alpha}$, $x_{3\to 0}^{\beta}$ and $x_{3\to 0}^{\gamma}$; in this work $x_{3\to 0}^{j} \cong 1 \times 10^{-30}$ is set. Note the difference between $x_{i,\infty}^{j}$ and $x_{i\to 0}^{j}$. The initialization scheme based on eq (A.1.1) and (A.1.2), is consistent with the values of the equilibrium ratios (or distribution coefficients) of component 3 when infinitely diluted in the binary three-phase system.

In this way, an initial value has been assigned to all the variables of the first T-3PP of the T-3PL to be built. The specifications for converging the first T-3PP are the mole fraction of component 3 in one of the phases (which is set equal to an extremely low value) and some other variable such as, e.g., the temperature for the case of an isothermal T-3PL (being such temperature indeed equal to that of the B-3PP).

After convergence is achieved for the T-3PP, the calculation of the T-3PL is initiated with the help of a numerical continuation method.

A.2-Starting off from a T-CEP contained in the T-3PL

A T-CEP with known numerical values for its variables is useful to obtain a T-3PP where two of the phases are quasi-critical. This T-3PP can be named "quasi-critical T-3PP" (qc-T-3PP). In a T-CEP two phases coexist in equilibrium, a critical phase with a non-critical phase. The variables that characterize a T-CEP are: T, P, V^c, V^{α}, x_1^c, x_2^c, x_3^c, x_1^{α}, x_2^{α}, x_3^{α}, u_1, u_2, u_3 *and* λ. T is the absolute temperature, P is the absolute pressure, V^j is the molar volume of phase j, and x_i^j is the mole fraction of component i in the phase j, with $i = 1.3$ and j=c or j=α. The superscript "c" refers to the critical phase, and the superscript "α" refers to the non-critical phase. u_1, u_2 *and* u_3 are the three components of certain eigenvector related to the critical conditions to be satisfied by the ternary critical phase present in the T-CEP, and λ is the eigenvalue associated to such eigenvector. The variables u_1, u_2 *and* u_3 provide useful information for the calculation of a qc-T-3PP (described below). Details about the conditions that must be satisfied to compute a ternary critical point and a T-CEP are given in Refs. [11,19].

Initializing variables to calculate a qc-T-3PP using the information from a T-CEP is relatively more complex than the procedures presented in sections 5 and A.1. The values of temperature (T) and pressure (P) of the qc-T-3PP are set equal to those of the known T-CEP. And the values of molar volume (V^{α}) and of mole fractions x_1^{α}, x_2^{α} and x_3^{α} of the (far from critical) phase "α" of the qc-T-3PP are set equal to the corresponding values of the variables of the phase α (noncritical phase) present in the known T-CEP.

To produce a qc-T-3PP, the critical phase of the T-CEP is taken to a condition where it splits into two quasi-critical phases (phases β and γ), having compositions close to that of the critical phase of the T-CEP. To achieve this separation, it is necessary to estimate the direction (in the mole fractions space) along which it occurs. This would be somewhat complicated for the case of ternary mixtures, since the tie-line connecting the compositions of phases β and γ, could have, at first sight, any direction. However, a direction chosen at random will in most cases lead to a lack of convergence. To estimate the compositions of the quasi-critical phases, the following equations are used:

$$x_i^{\beta} = x_i^c + s u_i \sqrt{x_i^c} \quad i = 1..3 \tag{A.2.1}$$

$$x_i^{\gamma} = x_i^c - s u_i \sqrt{x_i^c} \quad i = 1..3 \tag{A.2.2}$$

where x_i^{β} and x_i^{γ} are the unknown mole fractions of component i in phase β and phase γ of the qc-T-3PP, respectively, and x_i^c is the known mole fraction of component i in the critical phase "c" of the T-CEP. u_i is a known component of the eigenvector mentioned above, and "s" is a distance parameter that is set in this work equal to a value of about 1×10^{-5}. Eigenvector $\vec{u}$ is the direction along which the split of the critical phase is to be carried out.

Once the values for the mole fractions of each component in the phase "β" and phase "γ" are obtained from eq (A.2.1) and (A.2.2), V^{β} and V^{γ} are calculated at the temperature and pressure of the T-CEP using the chosen EOS (SRK-EOS [14] in this work). At this point all variables of the qc-T-3PP have initial values assigned. Next, the qc-T-3PP point is converged. To do so, the specified variable is, in this work, chosen to be the ratio of molar volumes V^{α}/V^{β} of the quasi-critical phases. This ratio is set equal to a value close to unity, e.g., 0.9995. This value makes possible to avoid the trivial solution during the process of converging the qc-T-3PP, since it forces the quasi-critical phases to be different, while keeping their properties very similar. The second degree of freedom to be specified is, in general, the temperature or the pressure, which indeed equals, respectively, the temperature or the pressure of the T-CEP. This variable is the one that remains constant along the T-3PL to be computed.

With this qc-T-3PP already converged and with the help of a numerical continuation method, the complete T-3PL is calculated.

A.3-Starting off from a binary critical end point (B-CEP) to which the T-3PL tends

In a B-CEP two phases coexist in equilibrium, a critical phase and a non-critical phase. The variables that characterize a B-CEP are: T, P, V^c, V^{α}, x_1^c, x_2^c, x_1^{α}, x_2^{α}, u_1, u_2 and λ. The conditions that must be satisfied to compute a binary critical point or a B-CEP will not be treated in this work (see Ref. [4]), although, these conditions are similar to those for the calculation of a T-CEP. The mentioned variables are the same than those of a T-CEP with the difference that x_3^c, x_3^{α} and u_3 corresponding to the third component are not present in the B-CEP. The information available in a converged B-CEP is useful to obtain a qc-T-3PP for which the third component is at significantly high dilution. We refer to such point as ID-qc-T-3PP (infinity dilution - quasi critical – T-3PP).

The first step consists of obtaining a converged quasi-critical binary three-phase point (qc-B-3PP) from the known B-CEP. This is done by applying the procedure of section A.2, except that now the number of components is two instead of three. Since the converged qc-B-3PP is a known B-3PP, the procedure of section A.1 is applied to obtain a T-3PP with very low component 3 concentrations in the system's phases, and with a couple of phases having very similar composition and density (qc-T-3PP).

A.4-Starting off from a ternary critical end point of a four phase line (T-CEP-4PL) to which the T-3PL tends

In a T-CEP-4PL three phases coexist in equilibrium, a critical

phase with two non-critical phases. The variables that characterize a T-CEP-4PL are: T, P, V^c, V^α, V^β, x_1^c, x_2^c, x_3^c, x_1^α, x_2^α, x_3^α, x_1^β, x_2^β, x_3^β, u_1, u_2, u_3 and λ. The superscript "c" means 'critical phase', and the superscripts "α" and "β" refer to the non-critical phases.

Phases "c" and "α" satisfy, if considered together, the conditions of a T-CEP, since a T-CEP is an equilibrium situation between a critical phase and a non-critical phase. Hence, the computation of a T-3PL can be, in principle, started off from the information in phases "c" and "α", as described in section A.2. The same is true for the pair of phases "c" and "β". We will identify these T-3PLs as T-3PL-αc and T-3PL-βc. The suffixes $-\alpha$c and $-\beta$c refer to the way in which the T-3PLs are calculated, i.e., by generating, as a first step (in the process of obtaining a first T-3PP), two quasi-critical phases from phase "c". Actually, this critical phase "de-stabilization" step needs to be done only once, and the result then used for both T-3PLs (T-3PL-αc and T-3PL-βc).

At a T-CEP-4PL two T-CELs and a T-4PL meet. This is always so (see Fig. 1).

It seems at first sight that the T-3PL-αc and the T-3PL-βc should always be calculable. However, for a given T-CEP-4PL, whether both T-3PLs (T-3PL-αc and T-3PL-βc), or only one of them, or none of them, are calculable, seems to depend on the relative angles (seen, say, in the PT plane) at which the T-CELs and the T-4PL reach the T-CEP-4PL; and also on the T-3PL specification, e.g., the T-3PL-αc and the T-3PL-βc could be set to have the same temperature than that of the T-CEP-4PL, or, otherwise, set to have, e.g., the same pressure than that of the T-CEP-4PL. For instance, the isobaric T-3PL(V) (say, that this is the T-3PL-αc) in Fig. 3 of the main text originates at the T-CEP-4PL: but there is no isobaric T-3PL-βc, or, in other words, such isobaric T-3PL-βc has a null length.

It is important to bear in mind that the T-3PL-αc is such that two of its three phases become identical when the T-3PL-αc reaches the T-CEP-4PL, being this point the termination point of T-3PL-αc. The same is true for T-3PL-βc. An example of this kind of T-3PLs is shown in Fig. 14 of the main text.

A third T-3PL, which we name T-3PL-$\alpha\beta$c, is obtained by directly using the information from the three phases of the T-CEP-4PL, in a simultaneous way. This can be done since the T-CEP-4PL is an already converged T-3PP (with the special feature of having a phase that satisfies the critical conditions). Notice that the suffix $-\alpha\beta$c implies that the T-3PL computation does not require a step of de-stabilization of the critical phase "c", i.e., the suffix $-\alpha\beta$c refers to a way of calculating the T-3PL-$\alpha\beta$c that differs from the way indicated by suffixes $-\alpha$c and $-\beta$c in T-3PL-αc and in T-3PL-βc. The absence of a de-stabilization step makes the computation of the T-3PL-$\alpha\beta$c more straightforward than the calculation of T-3PL-αc and of T-3PL-βc.

The T-3PL-$\alpha\beta$c contains the T-CEP-4PL as one of its three-phase equilibrium points. However, the T-CEP-4PL does not set, for T-3PL-$\alpha\beta$c, its termination or origin, i.e., the T-CEP-4PL is not an endpoint of the T-3PL-$\alpha\beta$c. Although the computation of the T-3PL-$\alpha\beta$c will progress in a given direction with respect to the location of the T-CEP-4PL, T-3PL-$\alpha\beta$c will also be stable in the opposite direction. This may be regarded as surprising, but it is not. An interesting feature of the T-3PL-$\alpha\beta$c is the following: when, while moving along this line, the T-CEP-4PL is approached, none of the two phases of any of the three possible pairs of phases (of the ternary three-phase equilibrium) tend to be identical, in spite of the fact that one of the phases tends to be critical. Such phase has access to the critical state exactly at the T-CEP-4PL. Fig. 13 of the main text shows a T-3PL-$\alpha\beta$c. Fig. 15 of the main text simultaneously shows the two T-3PLs which originate a the T-CEP-4PL of system [B].

A.5-Starting off from a ternary tricritical point (T-TCP) contained in the T-3PL

The variables [10] that characterize a T-TCP are: T, P, V^c, x_1^c, x_2^c,x_3^c, u_1, u_2, u_3, w_1, w_2, w_3 and λ. The superscript "c" refers in this case to the tricritical fluid mixture. w_1, w_2, w_3 are the components of a certain [10] vector orthogonal to $\mathbf{u}$ (i.e., $\mathbf{u}^T\mathbf{w} = 0$). Since a T-TCP is an end point of a (properly specified) T-3PL, it seems, from the ideas of section A.2, that it should be possible to initialize the variables of a quasi-tri-critical T-3PP (qtc-T-3PP) from the information contained in a converged T-TCP. However, we have not yet found a way of doing so.

Differential perturbations (in the appropriate directions) set on the composition of a T-TCP would result in the separation of the tri-critical phase into three quasi-tri-critical phases, whose compositions would be used to estimate the molar volumes of such phases. This information would be used to initialize the calculation of the qtc-T-3PP. The differential perturbations could be realized in infinite directions, if only the T-TCP composition, out of the full known T-TCP information, were to be used in such perturbation step. If such directions are set at random, no convergence for the qtc-T-3PP is obtained.

Unfortunately, so far it was not possible to find a way of using the information contained in vectors u and w to develop a method to initialize the variables of a qtc-T-3PP.

Fig. 4 and B.4 show different projections of a T-3PL (T-3PL(VI)) which develops between a T-4PP and a T-TCP (the acronyms T-TCP and T-TCEP have identical meaning, see Table 1).

Appendix B. Additional charts showing a number of T-3PLs for system [A]

Fig. B.1 shows the temperature (T)-molar volume (V) projection of T-3PL (I) (system [A]) (see also Fig. 3). This line begins in a T-4PP (low temperature) of the T-4PL (see T-CM, Fig. 3). The critical phenomenon (high temperature) can be appreciated when the T-3PL (I) reaches the T-CEP(c). At this point L1 = L2 (Fig. B.1). At the minimum temperature in Fig. B.1 (T-4PP) the three-phase system is not globally stable and a 4th phase appears, whose molar volume is not indicated in Fig. B.1.

Fig. B.2 shows the T-3PL (II) (T-V projection, see also Fig. 2). This line begins in a B-3PP(CO_2+H_2O) of the B-3PL(CO_2+H_2O) at low temperature (Fig. 2). The T-3PL (II) reaches the T-CEP (e) at high temperature, where L1 and L2 become critical (L1 = L2).

By rising the pressure from 69.35 bar (Fig. B.2) to 76.17 bar (Figs. 6 and 7) the phases L2 and L3 of minimum temperature (B-3PP in Fig. B.2) become critical (at the B-CEP temperature in Figs. 6 and 7). The T-CEP(e) is not the same in Fig. B.2 and Fig. 6, as it is evident from the temperature values of the T-CEPs(e).

Fig. B.3 shows the T-3PL (V) (T-V projection, see also Fig. 3). This line begins at the T-CEP-4PL. The phases L2 and L3 are critical at the temperature of the T-CEP-4PL (Fig. B.3). As the temperature increases the phases L1, L2 and L3 coexist in equilibrium. When the T-3PL(V) reaches the T-CEP(c), L1 and L2 become critical (L1 = L2, Fig. B.3).

When pressure increases from 109.3 bar (Fig. B.1) to 109.6 bar (Fig. B.3) pressure, the phases L2 and L3 at the T-4PP temperature (Fig. B.1) become critical, as shown in Fig. B.3 at the temperature of the T-CEP-4PL. Notice that the temperature range of the T-3PL(II) (Fig. B.2) is much wider than the temperature ranges of T-3PL(I) in Fig. B.1 and T-3PL(V) in Fig. B.3.

Fig. B.4 shows the T-3PL (VI) (T-V projection). This line, also shown in Fig. 4, was calculated maintaining a specific linear relationship between temperature and pressure. This PT relationship is such the T,P coordinates of the T-TCEP (II) (Fig. 4) satisfy such relationship. The T-3PL(VI) begins in a T-4PP (low temperature) of the T-4PL (see T-CM, Fig. 4) and ends at the T-TCEP (II). When the T-3PL (VI) reaches the T-

TCP (II), the phases L1, L2 and L3 become identical simultaneously (L1 = L2 = L3, Fig. B.4). Notice that, in Fig. B.4, changing the temperature implies changing the pressure. In other words, Fig. B.4 is neither an isobaric nor an isothermal phase diagram.

There is a slight difference in Fig. B.4 between the maximum value of the molar volume of the L1 phase and the molar volume of the T-TCEP. This is attributed to numerical limitations related to this type of calculations. Note that Fig. 4 shows that the T-3PL (VI) tends exactly to the T-TCEP. This is because the specification imposes an exact match of the (previously known) T,P coordinates of the T-TCEP. Variables other than T and P show small numerical differences with respect to the expected known values, at T,P coordinates equal to those of the T-TCEP.

A second T-3PL (named T-3PL(VII), not shown in this work) different from T-3PL(VI) (of Fig. 4 and Fig. B.4) could be calculated under the same specification than that of T-3PL(VI), being, the T-3PL(VII), stable also at temperatures higher than the T-4PP temperature (readable in Fig. B.4). T-3PL(VII) corresponds to a three-phase combination at the T-4PP different from the one of the T-3PL(VI) (combination shown in Fig. B.4). Besides, the T-3PL(VII) does not end at the T-TCEP(II) shown in Fig. 4, in spite of the fact that the T-3PL(VII) has a T-3PP of T, P coordinates identical to those of the T-TCEP(II). The T-3PL(VI) and T-3PL(VII) belong to different T-3PSs (both surfaces originate at the same T-4PL). Finally, the T-3PL(VII) does not meet critical or tri-critical conditions at the T,P values of the T-TCEP(II).

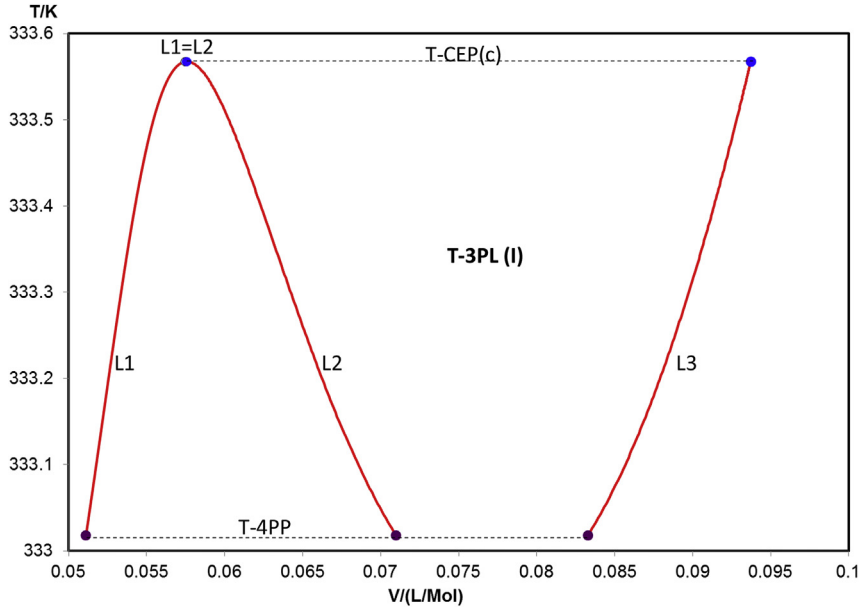

Fig. B.1. Temperature-Molar Volume projection of the calculated T-3PL(I) (P = 109.3 bar). See Fig. 3 and compare with Fig. B.3. System: *CO_2(1)+H_2O(2)+2-propanol(3)* [A]. Model: SRK-EoS (see Table 4). The T-CEP(c) indicated in this figure is not the same than that of T-3PL(III) and T-3PL(V) (see Fig. 3). Labels: T-CEP: Ternary-critical end point. T-3PL: Ternary three-phase line. T-4PP: Ternary four-phase point. Phase condition associated to labels: Table 2. Important: See note in Table 4.

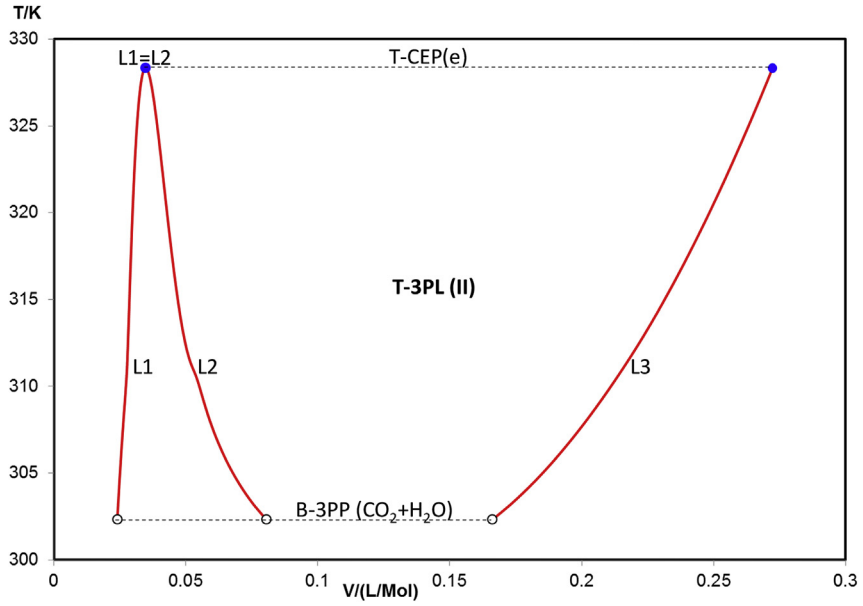

Fig. B.2. Temperature-Molar Volume projection of the calculated T-3PL(II) (P = 69.35 bar). Compare to Fig. 6 and see Fig. 2. System: *CO_2(1)+H_2O(2)+2-propanol(3)* [A]. Model: SRK-EoS (see Table 4). Labels: T-CEP: Ternary-critical end point. T-3PL: Ternary three-phase line. B-3PP: Binary three-phase point. Phase condition associated to labels: Table 2. Important: See note in Table 4.

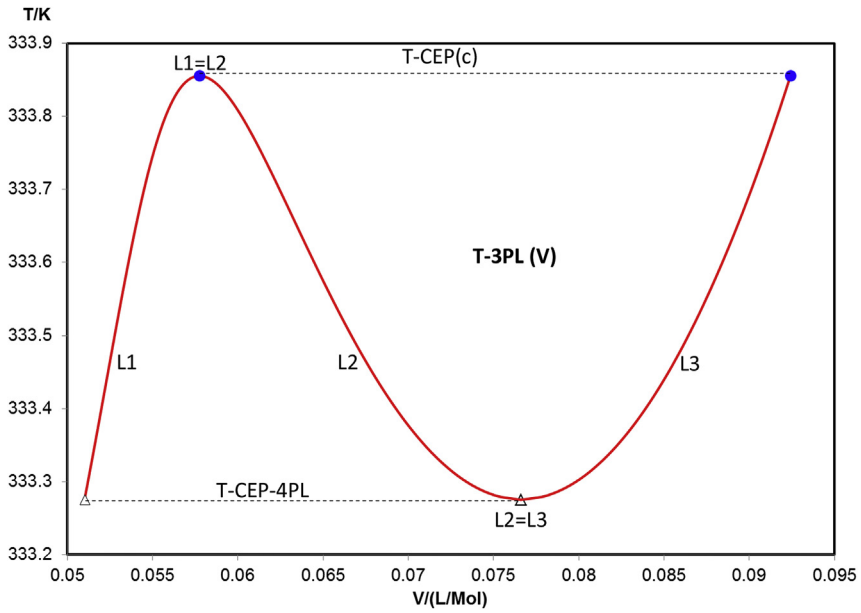

Fig. B.3. Temperature-Molar Volume projection of the calculated T-3PL(V) (P = 109.6 bar). See Fig. 3 and compare with Fig. B.1. System: *CO_2(1)+H_2O(2)+2-propanol(3)* [A]. Model: SRK-EoS (see Table 4). The T-CEP(c) is the same than the T-CEP(c) indicated in Figs. 3 and 5. The molar volume of the third phase of the T-CEP-4PL is not indicated in this figure. Labels: T-CEP: Ternary-critical end point. T-3PL: Ternary three-phase line. T-CEP-4PL: Ternary-critical end point of a four phase line. Phase condition associated to labels: Table 2. Important: See note in Table 4.

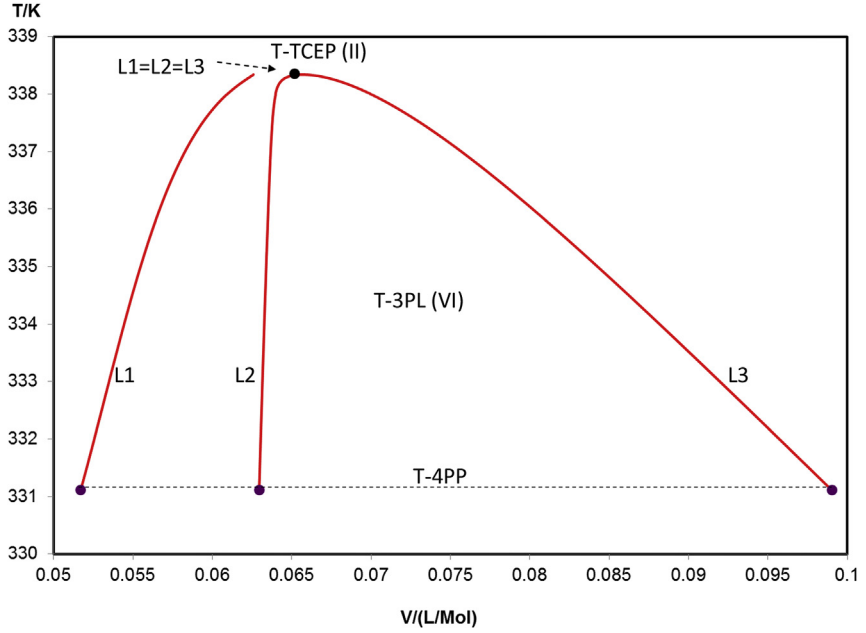

Fig. B.4. Temperature-Molar Volume projection of the calculated T-3PL(VI).
System: *CO_2(1)+H_2O(2)+2-propanol(3)* [A]. Model: SRK-EoS (see Table 4). A linear relationship between temperature and pressure remains valid along this T-3PL. The T-3PL specification is the following: $P = aT + b$ where a=(*1.8841 bar/K*) and b=(*-519.04 bar*). See Fig. 4. Labels: T-TCEP: Ternary-tricritical end point. T-3PL: Ternary three-phase line. T-4PP: Ternary four-phase point. Phase condition associated to labels: Table 2. Important: See note in Table 4.

References

[1] D. Kundu, T. Banerjee, Multicomponent vapor–liquid–liquid equilibrium prediction using an a priori segment based model, Ind. Eng. Chem. Res. 50 (2011) 14090–14096.
[2] B.D. Kelly, A. de Klerk, Modeling vapor–liquid–liquid phase equilibria in Fischer–Tropsch Syncrude, Ind. Eng. Chem. Res. 54 (2015) 9857–9869.
[3] R.L. Scott, P.H. van Konynenburg, Static properties of solutions: van der Waals and related models for hydrocarbon mixtures, Discuss. Faraday Soc. 49 (1970) 87–97.
[4] M. Cismondi, M.L. Michelsen, Global phase equilibrium calculations: critical lines, critical end points and liquid-liquid-vapour equilibrium in binary mixtures, J. Supercrit. Fluids 39 (2007) 287–295.
[5] J.R. DiAndreth, J.M. Ritter, M.E. Paulaitis, Experimental technique for determining mixture compositions and molar volumes of three or more equilibrium phases at elevated pressures, Ind. Eng. Chem. Res. 26 (1987) 337–343.
[6] J. Gregorowicz, T.W. de Loos, J. de Swaan Arons, Three-phase equilibria in the binary system ethylene+eicosane and the ternary system propane-+ethylene+eicosane, J. Chem. Eng. Data 38 (1993) 417–421.
[7] S. Winkler, K. Stephan, Fluid multiphase behavior in ternary mixtures of CO2, H2O and 1-butanol, Fluid Phase Equilibria 137 (1997) 247–263.
[8] T. Adrian, H. Hasse, G. Maurer, Multiphase high-pressure equilibria of carbon

dioxide-water-propionic acid and carbon dioxide-water-i sop ropanol, J. Supercrit. Fluids 9 (1996) 19–25.
[9] T. Adrian, S. Oprescu, G. Maurer, Experimental investigation of the multiphase high-pressure equilibria of carbon dioxide+water+(1-propanol), Fluid Phase Equilibria 132 (1997) 187–203.
[10] G. Pisoni, M. Cismondi, L. Cardozo-Filho, M.S. Zabaloy, Generation of characteristic maps of the fluid phase behavior of ternary systems, Fluid Phase Equilibria 362 (2014) 213–226.
[11] G. Pisoni, M. Cismondi, L. Cardozo-Filho, M.S. Zabaloy, Critical end line topologies for ternary systems, J. Supercrit. Fluids 89 (2014) 33–47.
[12] G.O. Pisoni, S.B. Rodriguez-Reartes, J.I. Ramello, M. Cismondi, M.S. Zabaloy, A study on the effect of ternary interaction parameters on the equation of state description of ternary fluid phase equilibria, Fluid Phase Equilibria 391 (2015) 54–66.
[13] M. Cismondi, M.L. Michelsen, M.S. Zabaloy, Automated generation of phase diagrams for binary systems with azeotropic behavior, Ind. Eng. Chem. Res. 47 (2008) 9728–9743.
[14] G. Soave, Equilibrium constants from a modified Redlich-Kwong equation of state, Chem. Eng. Sci. 27 (1972) 1197–1203.
[15] E.L. Allgower, K. Georg, Introduction to Numerical Continuation Methods, SIAM. Classics in Applied Mathematics, Philadelphia, 2003.
[16] Y.S. Wei, R.J. Sadus, Critical transitions of ternary mixtures: a window on the phase behavior of multicomponent fluids, Int. J. Thermophys. 15 (1994) 1199–1209.
[17] R.J. Sadus, Novel high pressure critical phase transitions in multicomponent fluid mixtures, Fluid Phase Equilibria 83 (1993) 101–108.
[18] R.J. Sadus, Novel critical transitions in ternary fluid mixtures, J. Phys. Chem. 96 (1992) 5197–5202.
[19] M.L. Michelsen, J.M. Mollerup, in: E.H. Stenby (Ed.), Thermodynamic Models: Fundamentals and Computational Aspects, Tie-Line Publications, 2007.
[20] T. Adrian, M. Wendland, H. Hasse, G. Maurer, High-pressure multiphase behaviour of ternary systems carbon dioxide-water-polar solvent: review and modeling with the Peng-Robinson equation of state, J. Supercrit. Fluids 12 (1998) 185–221.
[21] J.R. Di Andreth, Multiphase Behavior in Ternary Fluid Mixture, Ph. D. Tesis, Department of Chemical Engineering, University of Delaware, Delaware, USA, 1985, p. 164.
[22] R. Privat, R. Gani, J.-N. Jaubert, Are safe results obtained when the PC-SAFT equation of state is applied to ordinary pure chemicals? Fluid Phase Equilibria 295 (2010) 76–92.
[23] J.O. Valderrama, The state of the cubic equations of state, Ind. Eng. Chem. Res. 42 (2003) 1603–1618.
[24] Y.S. Wei, R.J. Sadus, Equations of state for the calculation of fluid-phase equilibria, AIChE J. 46 (2000) 169–196.
[25] R.J. Sadus, Calculating critical transitions of fluid mixtures: theory vs. experiment, AIChE J. 40 (1994) 1376–1403.
[26] Ø. Wilhelmsen, A. Aasen, G. Skaugen, P. Aursand, A. Austegard, E. Aursand, M.A. Gjennestad, H. Lund, G. Linga, M. Hammer, Thermodynamic modeling with equations of state: present challenges with established methods, Ind. Eng. Chem. Res. 56 (2017) 3503–3515.
[27] I. Polishuk, A. Mulero, The numerical challenges of SAFT EoS models, Rev. Chem. Eng. 27 (2011) 241–251.
[28] E. Wiberg, N. Wiberg, Inorganic Chemistry, Academic Press, 2001.
[29] E. Brandt, E. Ulrich Franck, Y.S. Wei, R.J. Sadus, Phase behaviour of carbon dioxide-benzene-water ternary mixtures at high pressures and temperatures up to 300 MPa and 600 K, Phys. Chem. Chem. Phys. 2 (2000) 4157–4164.
[30] J.M. Milanesio, M. Cismondi, L. Cardozo-Filho, L.M. Quinzani, M.S. Zabaloy, Phase behavior of linear mixtures in the context of equation of state models, Ind. Eng. Chem. Res. 49 (2010) 2943–2956.
[31] R.L. Rowley, W.V. Wilding, J.L. Oscarson, Y. Yang, N.A. Zundel, T.E. Daubert, R.P. Danner, Data Compilation of Pure Compound Properties (DIPPR), 2003.